BIOMECHANICAL MODELING OF THE MASTICATORY REGION

A Thesis Submitted to the College of

Graduate Studies and Research

In Partial Fulfillment of the Requirements

For the Degree of Master of Science

In the Department of Computer Science

University of Saskatchewan

Saskatoon

By

Benedikt Sagl

PERMISSION TO USE

In presenting this thesis in partial fulfilment of the requirements for a Graduate degree from the University of Saskatchewan, I agree that the Libraries of this University may make it freely available for inspection. I further agree that permission for copying of this thesis in any manner, in whole or in part, for scholarly purposes may be granted by the professor or professors who supervised my thesis work or, in their absence, by the Head of the Department or the Dean of the College in which my thesis work was done. It is understood that any copying or publication or use of this thesis or parts thereof for financial gain shall not be allowed without my written permission. It is also understood that due recognition shall be given to me and to the University of Saskatchewan in any scholarly use which may be made of any material in my thesis.

Requests for permission to copy or to make other use of material in this thesis in whole or part should be addressed to:

Head of the Department of Computer Science

University of Saskatchewan

Saskatoon, Saskatchewan (S7N 5C9)

ABSTRACT

Biomechanical simulation is an essential tool for the understanding of the human masticatory system, because many parameters and functions cannot be studied *in vivo* due to the invasiveness of their examination methods. Previous simulation studies include investigations of the masticatory cycle [1], the joint forces during opening and closing of the jaw [2] and distraction osteogenesis [3]. In this thesis we present projects that aim to increase the understanding of the masticatory system as well as to increase the availability of computational jaw models.

We present a new optimization approach for inverse simulations that incorporates constraint reaction forces into the inverse solver. This method was used to develop an inverse dynamic biomechanical simulation of sleep bruxism. We also developed a detailed model of the sub compartments of the lateral pterygoid muscle, which we used to derive a theory that explains previously published EMG patterns during a contralateral movement of the mandible. Lastly, we investigated possible ways to port the ArtiSynth jaw model to OpenSim, which would increase its availability tremendously.

To show that our optimization approach works correctly and enables us to set a predefined level of reaction force, we computed multiple simple simulations using a test model as well as an upper extremity model. Using a movement goal as well as a bite force goal we are able to realistically simulate teeth grinding behavior. Our simulations predict that bilateral masseter muscle activation is mainly concerned with the creation of closing force, while unilateral temporalis muscle activation is used to create the movement, necessary for tooth grinding. Due to the simulation set up submental activation could not be simulated, even though it is reported in literature. The simulation results for our new lateral pterygoid model show good

agreement with activation recordings gathered using electromyography. Furthermore we developed a way to port muscle properties from ArtiSynth to OpenSim and designed a new representation of the temporomandibular joints that only uses one joint. Preliminary tests of dynamic jaw simulations in OpenSim show promising results. Together the contributions reported in this thesis have extended the capability and availability of biomechanical jaw modeling.

ACKNOWLEDGMENTS

Firstly I want to express my sincere gratitude to my advisor Prof. Stavness, who introduced me to the world of biomechanical modeling. He encouraged me to transfer to the University of Saskatchewan where he always made me feel more than welcome. His guidance helped me in all phases of my research and due to his support I was able to travel to many new destinations during my stay at his lab. Also I'm grateful to my colleagues and friends, who made my stay in Saskatoon an experience I will cherish for the rest of my life.

My sincere thanks goes to Prof. Slavicek, who introduced me to the fascinating system that is the masticatory apparatus and who enabled and encouraged my desire for scientific work. Furthermore I want to thank him for always being willing to share his expertise in the field of dentistry with me. Our discussions have always been extremely helpful.

Also I would like to thank the Rudolf Slavicek- Siegfrid Ludwig Stipend Fund for helping me accomplish my scientific goals over the last few years by providing me with financial support.

I want to thank my family for all the support and love I received, even though they were a continent away. Especially I want to thank my parents whose guidance and help made my accomplishments possible. Lastly, I want to thank my girlfriend Melanie for supporting my decision to take this opportunity, for helping me through hard times and for always being on my side, even if it was 2am in Vienna.

TABLE OF CONTENTS

LIST OF TABLES

LIST OF FIGURES

Figure page

CHAPTER 1:
INTRODUCTION

The masticatory apparatus is a very complex system that is used constantly for fundamental tasks of our everyday life, including eating, breathing and speaking. Dysfunctions of the masticatory system could lead to severe problems like speech impairment or inability to chew. Common dysfunctions include bruxism and temporomandibular joint disorders. Dental and orthodontic procedures to reshape, reposition and replace teeth can significantly alter the mechanics of the jaw system and the way in which people chew, hence these everyday procedures could lead to the development of temporomandibular joint problems. Biomechanical investigations of the impact of these procedures could lead to a reduced amount of complications, and hence directly benefit the patient.

Dysfunctions of the jaw region and the dentition can lead to a range of problems with the temporomandibular joint (TMJ), which connects the skull with the mandible. These disorders are grouped as temporomandibular joint disorders (TMD). TMD is commonly found in patients between the age of 20-40 and studies found a prevalence of 20-25% among the population of the United States [4]. Even though a large group of the population is affected by TMD, there is little consensus on the causes underlying TMD. The lack of understanding can be attributed to the high complexity of the TMJ, which is the only human system that is composed of two joints that connect the same two bony structures, namely the skull and the mandible, and the large number of muscles within the small region of the masticatory system. Moreover, the temporomandibular

joint contains a soft-tissue disk that, from a functional point of view, splits the joint into two separate units.

Another important dysfunction of the jaw region is sleep bruxism, which is characterized by involuntary repetitive grinding and clenching of teeth while asleep. 64-84% percent of sleep bruxism patients experience orofacial pain as well as an increased amount of headaches [5]. Furthermore, bruxism can lead to severe abrasion of teeth that can go so far as patients completely losing their tooth crowns. These patients will face major challenges during fundamental tasks like mastication. It has also been speculated that bruxism may increase the load that is applied to the temporomandibular joints, which may be associated with temporomandibular disorders [5].

TMD as well as bruxism are prevalent dysfunctions, but are currently not fully understood. To get more insight on various malfunctions of the masticatory system, it is important to understand the muscle forces that are created, since the muscles apply the loads that lead to the various problems, such as tooth abrasion during bruxism. Additionally, an increase of muscle force will automatically increase the load on the TMJ, which is of relevance for the development of TMD. Hence a thorough investigation of muscle force vectors, muscle force magnitudes and the muscle activation patterns during different functions and dysfunctions could lead to new insight in various problems of the jaw region.

Unfortunately, measuring *in vivo* data of the jaw region poses some problems. Even recording jaw movement data is not as simple as expected, since placing markers on the skin does not record the movement of the mandible appropriately.

The most common, noninvasive method for the investigation of muscle activation is electromyography (EMG). EMG records the electrical activity produced by muscles during

contraction. To diagnose sleep bruxism overnight EMG recordings are screened to detect repetitive, rhythmic masticatory muscle activity (RMMA) of the masseter and temporal muscles [5].

EMG acquisition is difficult for small or deep muscles of the masticatory system, since it often struggles with the problems that occur due to the huge amount of muscles located in the small area of the jaw region [6]. The abundance of muscles makes the placement of EMG electrodes a complicated task, and even with correctly placed electrodes, the problem of recording signals from multiple overlaying muscles remains unsolved. Furthermore, it is difficult to record EMG data for multiple muscles at the same time, without interference between the separate recordings.

Bite forces are another important variable of biomechanical simulations. They can be used to distinguish the amount of muscle activation in a system as well as to distinguish the load that is applied to the temporomandibular joint. Measuring bite forces is also a very challenging task, since even a small force transducer changes the way a patient is biting and therefore will not measure the physiological level of bite force [7].

Computer simulations of the masticatory system have been used more frequently in recent years to work around all the problems of a highly complex anatomical system and limited ability to perform *in vivo* measurements of the jaw muscles [8]. In particular, the use of inverse dynamics simulations with a musculoskeletal jaw model could possibly lead to valuable insight in the workings of different problems of this region, since these simulations predict muscle function and force loads from only very basic input data, such as jaw motion and bite forces.

Problem

Even though biomechanical simulations of the masticatory region are a promising field, there are still some major limitations left that need to be solved to increase their impact and usability.

First of all, most dynamic models of the jaw region are trying to find a very simple representation of all components of the system. While this approach is sufficient for many studies, sometimes more complicated models of the TMJ or a specific muscle are needed. Muscles, for example, are often represented as simple point-to-point muscles that have only a single point modeling their origin and insertion, instead of an area [1][2][3]. Obviously, this can lead to problems for muscles that have a large insertion area or for muscles that are composed of multiple sub compartments with different muscle force vectors.

Another problem with biomechanical simulations of the jaw region is their availability for scientific research. Most models are either not publicly available or developed in a commercial software package [2][3][9]. This issue makes it difficult to increase the number of people that are working in the area of orofacial biomechanics, since there are quite large obstacles at the beginning of a project.

As described above, bite forces play an important role in biomechanical simulations of the jaw region. In general, musculoskeletal modeling reaction forces (such as the force between the foot and ground during walking) would be measured and then played back as external forces into a simulation [10]. However, as discussed earlier, measuring bite force is very challenging. Moreover the use of external forces can lead to unstable simulations, since the reaction forces are not included in the optimization process, which makes the investigation of high force tasks tedious and unreliable.

Another limitation of current investigations of the masticatory system is the lack of detailed modeling set-ups for different dysfunctions. Due to the fact that all biomechanical models need simplifications to simulate within a reasonable time frame, it is necessary to alter a generic model accordingly to look at a specific problem in detail. To fully understand different causes for problems of the masticatory system, we need specialized models and simulation workflows. [8]

Objectives

This thesis describes a number of modeling innovations and simulation-based experiments to showcase solutions for the various problems we described above. We have developed and evaluated models as well as optimization methods.

The first objective of this thesis was to create a new, more detailed model of the lateral pterygoid muscle that incorporates different sub compartments of the muscle. Furthermore, we wanted to adapt the Hannam et al. jaw model to create a specialized model that was used to create an inverse dynamics simulation of sleep bruxism [1].

To enable a sleep bruxism simulation, we planned on developing a new quadratic term that incorporates constraint reaction forces into the optimization of an inverse dynamics simulation. To test this new optimization term a series of simple simulations should be developed.

We planned to create these simulations using the modeling toolkit ArtiSynth that contains a publicly available model of the masticatory region that was already used for various publications in the field of masticatory biomechanics [1][11]. This should make our newly implemented methods easily accessible. To increase the model's availability, our last objective

was to work on implementing the Hannam et al. jaw model in OpenSim, which is the world's most used musculoskeletal modeling toolkit [10].

Contributions

This thesis will highlight the author's contributions to the projects presented earlier.

Detailed Lateral Pterygoid Muscle Model

For the lateral pterygoid project, a new model of the sub-compartments of the muscle was created according to recent anatomical literature [12][13]. Inverse simulations of lateral jaw movement were performed and compared to EMG studies [14][15][16][17][18][19][20][21]. Our interpretation of the simulation results led to a new biomechanical theory for the working of the lateral pterygoid muscle's sub compartments.

OpenSim Implementation of the Jaw Model

Our goal was to port our biomechanical jaw model to OpenSim, the most widely used simulation platform in the world [10]. To port the ArtiSynth model to OpenSim two major problems had to be overcome. First of all, the two toolkits use different muscle models, hence a way to port the muscle properties, while conserving the behavior of the muscles, had to be found. Additionally, the differences in joint representation made it impossible to use the ArtiSynth joint model in OpenSim. To solve this problem, we proposed and evaluated two different ways to model the temporomandibular joint in OpenSim.

Development of a new Reaction Force Optimization Term

To enable the user to easily incorporate reaction forces into the inverse simulation workflow, a new quadratic optimization term was developed. To validate our implementation, a test case was created and simple simulations were computed. Furthermore, we tested the implementation using an upper extremity model to show its general applicability.

An Inverse Dynamics Simulation of Sleep Bruxism

The main contribution of this thesis was to develop an inverse dynamics simulation of sleep bruxism. To our knowledge, this is the first biomechanical simulation based investigation of the muscle activations in sleep bruxism. For this purpose, we adapted the Hannam et al. model and ran various inverse simulations. Furthermore, we evaluated the muscle activation levels predicted by the simulation in different bruxism contexts, e.g. the effect of grinding on the canine tooth compared to the first molar.

Outline

In this thesis, I will present the results of various projects that highlight different approaches of biomechanical simulations to the jaw region.

Chapter 2 presents background information on topics that are necessary for the understanding of the following chapters of this thesis. This includes descriptions of the different muscles, bones and joints that compose the masticatory region.

Furthermore, previous biomechanical models will be presented. This should give a rough understanding of different ideas that were used to model parts of the system, for example the temporomandibular joint.

A significant emphasis of this thesis is the development of a biomechanical simulation of sleep bruxism. Therefore an overview of the dental literature on bruxism will be given to highlight the problems connected with this malfunction.

Furthermore, the ArtiSynth modeling toolkit and its features will be presented, along with some selected papers that used this toolkit to investigate different tasks of the masticatory system.

Our main idea was to create an inverse dynamics simulation of sleep bruxism. Since jaw movement alone is not enough information to define a teeth grinding task, we developed a new inverse simulation approach that uses a reaction force goal that makes it possible to set a predefined constraint force level. Using a constraint as tooth contact model, this enables us to create an inverse dynamics bruxism simulation without the use of external forces. The reaction force goal will be explained in detail in chapter 3 and our findings on bruxism are presented in chapter 4.

Additionally, we created a new model of the sub compartments of the lateral pterygoid muscle. Murray et al. have reported many detailed experimental EMG measurements for sub compartments of the lateral pterygoid during lateral jaw movements, but provide little information on possible reasons for these data [14]. To develop a theory that could explain these findings from a biomechanics perspective, we ran inverse dynamics simulations for a lateral movement using our new detailed model of the lateral pterygoid. We present our findings on these muscle activation patterns in chapter 5.

Furthermore, we investigated various possibilities to transfer the ArtiSynth jaw model to the OpenSim simulation toolkit, because it currently lacks a jaw. This is mostly due to the fact that OpenSim only allows one joint between two bodies, hence the modeling of the left and right

temporomandibular joints is a very challenging task. Moreover, OpenSim is using a different muscle model than ArtiSynth, which on the one hand offers new possibilities for investigations of muscles, while also causing problems porting the "old" muscle properties. In chapter 6, we present two different approaches that could be used to create temporomandibular joints in OpenSim as well as a method to port the muscle properties.

Lastly, this thesis will outline various possibilities for improvements as well as future steps that could use the methods presented in this thesis to derive new insights into the workings of the masticatory system.

CHAPTER 2:
BACKGROUND

Anatomy of the Jaw Region

Since the masticatory apparatus is a very complex system, the anatomy that forms the region will be presented. This will include the bony structures that compose the system as well as the muscles of mastication and the human dentition. Understanding of the anatomy of the jaw region will be helpful to comprehend the workings of the biomechanical models and their different modeling approaches for various parts of the anatomy.

Bony Structures

The jaw region contains three bony structures: the skull, the mandible and the hyoid bone. The skull is composed of multiple smaller bones that fuse together in an early stage of human development. The maxilla, which is composed of two fused halves, is of special interest, because it holds the upper dentition and hence is of high importance for most tasks of the jaw region, including mastication, speech, clenching and grinding. Furthermore, the temporal bone plays a big role, since its processes are important muscle insertions. Additionally the mandibular fossa of the temporal bone is part of the temporomandibular joint.

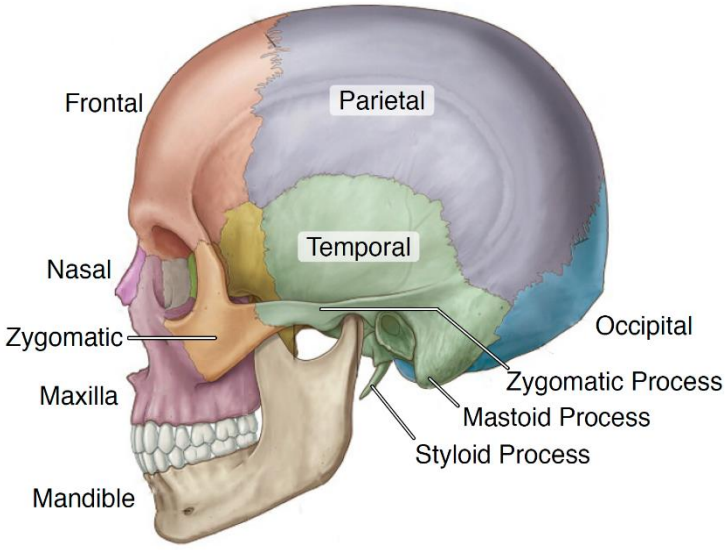

Figure 1: bony structures of the masticatory region (hyoid not included, ©Elsevier (2010), adapted with permission [22])

The second important bony structure, the mandible, is a u-shaped bone, which holds the lower dentition. It has two joints connecting both ends with the skull, via the condylar process. Many muscles of the region are connected to the mandible, which leads to a high mobility of the bone.

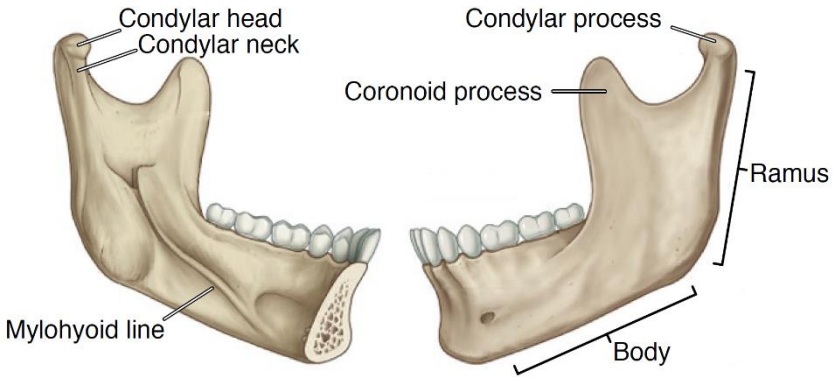

Figure 2: schematic drawing of the mandible (©Elsevier (2010), adapted with permission [22])

The hyoid bone is a small u-shaped bone situated roughly between the two mandibular arches. Its only connection to the jaw region is by muscles, which means it is not directly connected to any other bone. The main functions of the hyoid bone arise during swallowing and

breathing. In terms of the masticatory system it is important because a lot of jaw muscles are connected to the hyoid and can open the mouth, if the hyoid's position is stabilized by other muscles.

Dentition

The human dentition is composed of 32 teeth. Teeth shape can vary significantly from broadly shaped molars that are used to crush food to quite thin and sharp incisors that are used to bite off portions of food. Furthermore, the shape and number of dental roots, which couple the teeth to their containing bony structure, varies depending on their task. Figure 3 shows an overview of the human dentition.

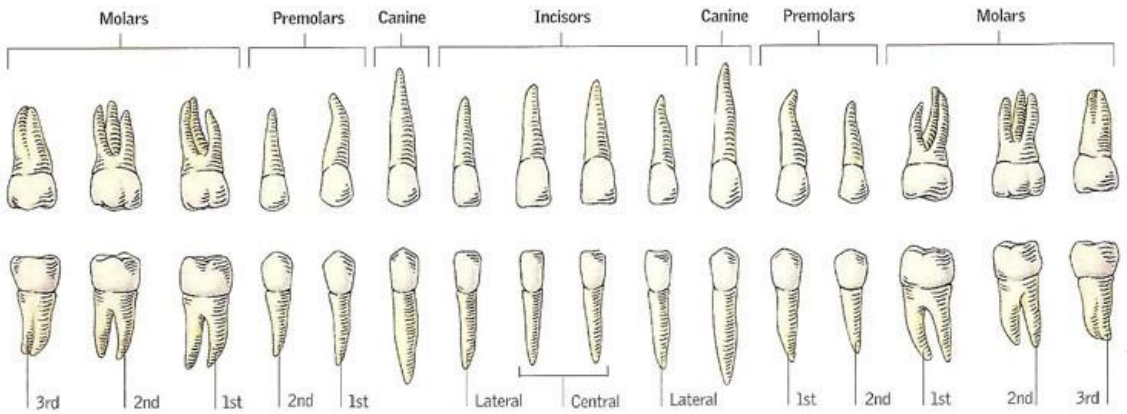

Figure 3: human dentition [23]

Temporomandibular Joint

The skull and the mandible are connected by two joints, one on each end of the mandible. These joints are called temporomandibular joints, because they connect the mandible with the temporal bone. The connection of two bony structures with two completely separate joints between them is a unique feature of the jaw region. The temporomandibular joint is a synovial joint, which means that the connective tissue around the joint forms a bag that is filled with fluid.

The most interesting feature of the joint is the temporomandibular disk. This disk separates the joint into two compartments with different movement tasks. The disc-temporal bone compartment is used for translation of the mandible, while the compartment between disc and mandible is used for rotation. The jaw is encapsulated by various tendons and is held in rest position by the passive forces of the closing muscles.

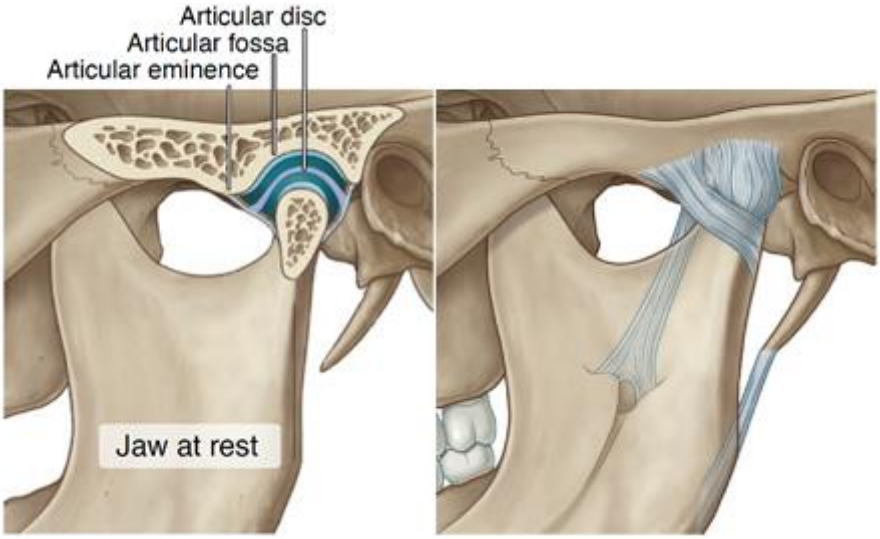

Figure 4: structures that compose the temporomandibular joint; encapsulated joint (©Elsevier (2010), adapted with permission [22])

Muscles of the Jaw Region

The muscles of the jaw region can be roughly separated into two groups, jaw opening and jaw closing muscles. The jaw closing muscles are the masseter, temporalis and medial pterygoid muscles and the opening muscles are the digastric, mylohyoid and lateral pterygoid muscles. All muscles described below are present on both sides of the skull and mandible.

The masseter muscle is a closing muscle that originates at the zygomatic arch and inserts at the ramus of the mandible and is one of the strongest muscles of mastication. It is separated into a superficial and a deep head with slightly different muscle force vectors.

The temporalis muscle is a fan shaped muscle with a wide area of origin over the lateral side of the skull. It inserts at the medial side of the ramus of the mandible. Due to its large area the force vector of the muscle can be varied significantly by strongly activating different parts of its area.

The last closing muscle is called medial pterygoid muscle and is composed of two heads, originating at the pterygoid fossa and inserting at the lower part of the medial side of the mandibular ramus.

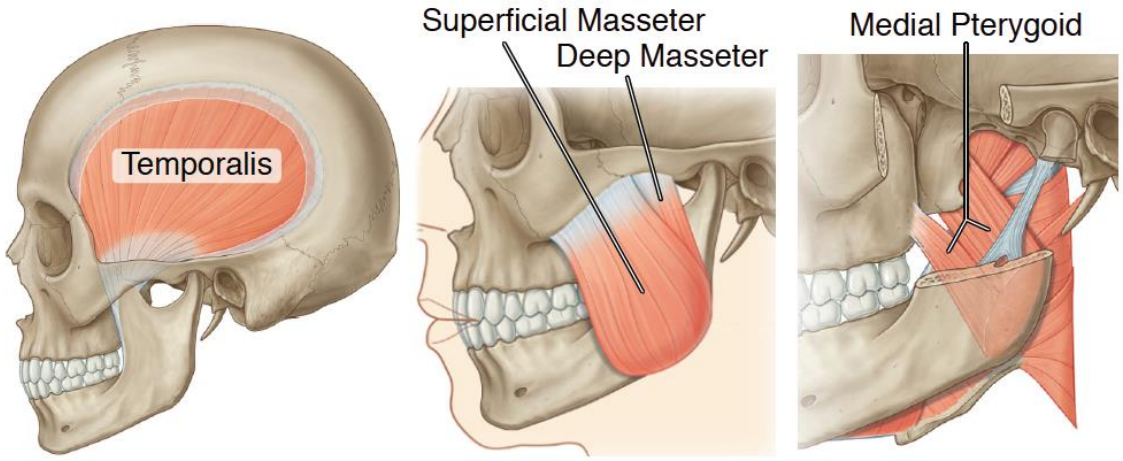

Figure 5: jaw closing muscles (©Elsevier (2010), adapted with permission [22])

The digastric muscle is composed of an anterior part spanning from the digastric fossa, close to the symphysis of the mandible, to the hyoid bone, while the posterior part connects the hyoid to the mastoid process of the temporal bone. Activating the anterior part of the digastric muscle, while fixing the position of the hyoid by using activation of multiples muscles, leads to an opening of the jaw.

The lateral pterygoid muscle is separated into two heads. The inferior head spans from the outer surface of the lateral pterygoid plate to the condyle, with parts inserting into the joint

capsule. The superior part originates at the sphenoid bone and inserts into the condyle and the capsule.

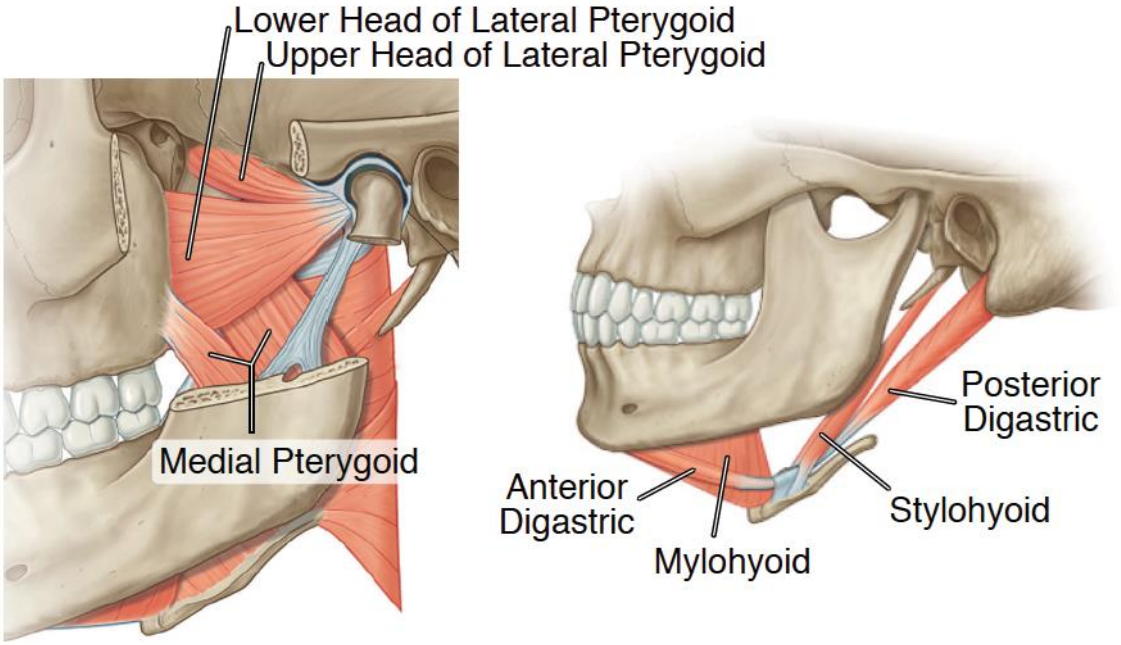

Figure 6: opening muscles of the jaw region, including digastric, mylohyoid and lateral pterygoid muscles (©Elsevier (2010), adapted with permission [22])

The mouth floor is built by the mylohyoid muscle that spans from the mandible to the hyoid bone and can act as a rather weak opening muscle. Figure 5 and figure 6 show schematic drawings of the closing and opening muscles of the jaw.

Sleep Bruxism

The glossary of prosthodontic terms defines bruxism as an oral parafunction characterized by involuntary grinding and clenching of the teeth [24]. Modern studies suggest that a further distinction between awake and sleep bruxism should be made, since it is likely that they have different physiological causes as well as different grinding and clenching patterns. In this thesis, we will focus on sleep bruxism. Sleep bruxism is found in 8% of the general adult population and in up to 40% of children under the age of 11 [5][25][26].

Sleep bruxism can lead to severe tooth wear and muscle hypertrophy [5]. In severe cases, this can go as far as the patient's loss of the ability to masticate food, since the tooth crowns are grinded completely flat. Furthermore this can lead to speech impairments of the patient. The increased loads on the temporomandibular joint, which occur due to the raised muscle activation, are often linked to temporomandibular joint disorders [4]. This group of disorders leads to pain in the joint between the mandible and the skull and can make the movement of the mandible very painful for the patient [4].

The best-practice for the diagnosis of sleep bruxism (SB) is the analysis of overnight EMG recordings. This is done by detecting repetitive, rhythmic masticatory muscle activity (RMMA) of the masseter and temporal muscles [5]. These RMMA patterns also occur in 60% of the general adult population, but their occurrence is 3 times higher in SB patients [27].

Since the detection of RMMA is quite challenging, dentists often have to look for severe grinding patterns on patient's tooth crowns or use recordings of tooth grinding sounds during the night [28]. Nevertheless the recording of RMMA events is the only reliable way to diagnose sleep bruxism.

The causes of sleep bruxism are mostly unknown. The possible reasons for the development of sleep bruxism include sleep arousal, autonomic sympathetic-cardiac activation, genetic predisposition, neurochemicals, psychosocial components, exogenous factors, and comorbidities [5]. Little information can be found on the role of the different jaw muscles except for the masseter and temporalis muscle. Lavigne et al. published EMG data of a polysomnographic recording in a sleep lab [29]. They report differential activation of the left and right temporalis muscle, with magnitudes switching at every bruxism event. Furthermore, they

report bilateral activation of the masseter with higher activation on the working side. They also describe co-activation of the submental muscles during bruxism.

Computer Modeling of the Jaw Region

The first biomechanical simulations of the masticatory system go back multiple decades. Greaves et al. investigated the effect of teeth placement on bite force creation of ungulates in a 2D model as early as 1978 [30]. Thockmorton et al. present an early 2D investigation of temporomandibular joint reaction forces in a two muscle model [31]. Since that time, numerous model and simulation approaches have been published. Modern biomechanical investigations of the jaw region include rigid body models as well as finite-element (FE) approaches. Examples of rigid body models are the Hannam et al. 2008 and the Tuijt et al. 2010 model [1][2]. Aside from the software environment, important differences between various rigid body models often include the representation of the temporomandibular joint. Tuijt et al. used shell type meshes to define the articular surface of the temporomandibular joint, while Hannam et al. used a combination of frictionless unilateral constraints.

Finite element models represent the components of a system as meshes of finite elements, e.g. triangles. Using this method, deformation and stresses on all parts of a structure can be investigated, although the creation of the mesh can be tedious and time consuming, because this method is very sensitive to the boundary conditions, element shape, shape size and material properties of the model [8]. Moreover, FE models need quite high computational power to compute. Röhrle et al. published an investigation of mastication forces using a detailed finite element model for the masseter muscles [32].

Rigid body simulations are modeling all hard tissues as non-deformable structures. Although this simplification might introduce some error, due to small deformations that occur *in*

vivo, multiple benefits occur as well. First of all, the additional error might be quite small, because a more complicated bone modeling approach needs additional material properties that could be very hard or impossible to measure, and hence an assumption of the parameter might introduce an error as well [8].

In general, rigid body models are especially useful for dynamic investigations, since the amount of required computational power is quite small, compared to e.g. FE investigations. By driving a rigid body model using muscle forces, various output parameters, like jaw movement, joint forces and bite forces, can be investigated.

Using muscle activations as input parameter of the simulation is called a forward simulation approach. Another interesting approach is called inverse simulation and uses movement trajectories of a body, e.g. the mandible, as input, since movement is easier to record than muscle activations themselves. A detailed explanation of these approaches can be found in Chapter 3.

Biomechanical models of the jaw region have been developed in various environments, including engineering toolkits, which are not primarily used for biomechanical investigations, as well as toolkits that were specifically developed for this kind of investigation. Examples include Matlab [2], AnyBody [3], Madymo [9] and ArtiSynth [1]. Some toolkits, like ArtiSynth and Madymo, enable the user to develop combined rigid body and FE models, which can increase the level of detail for areas of interest, while still keeping the computational burden at a reasonable level.

ArtiSynth Modeling Toolkit

Since all simulations presented in this thesis are either using ArtiSynth and its jaw model or trying to port the model from ArtiSynth to another toolkit we will briefly discuss the platform and the model itself.

ArtiSynth is an open-source modeling toolkit that was originally developed for biomechanical investigations of speech. Over the years, it has evolved into a toolkit that can be used for general biomechanical modeling, although a focus on biomechanics of the head and neck region remains [33]. One feature of particular interest is ArtiSynth's ability to incorporate rigid bodies as well as FE structures. This is especially promising for the jaw region, because this region incorporates many important hard and soft tissue components.

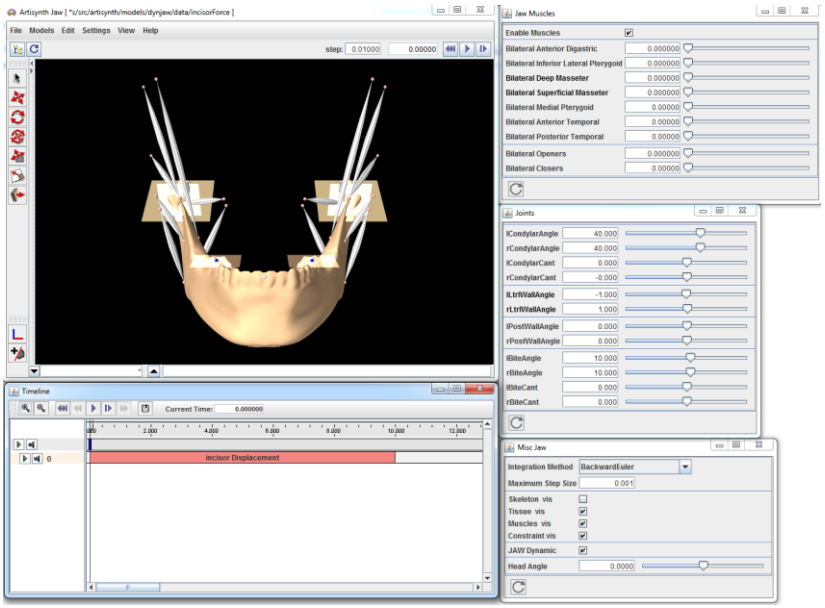

Figure 7: ArtiSynth with the Hannam et al. 2008 model loaded

The Hannam et al. 2008 model acts as base for all simulations presented in this thesis. The meshes of the bony structures were derived from CT data of a male subject and bone inertia data were gathered from earlier literature. Masses were estimated according to mesh size and

geometry and muscle insertions and origins were detected using anatomical landmarks. The temporomandibular joints were modeled using three frictionless surfaces that coincided with the anatomical center of the condyle. The surfaces were modeled as unilateral constraints, which enables the condyle to leave the constraints in one direction, while penetration of the surface in the opposite direction was prohibited.

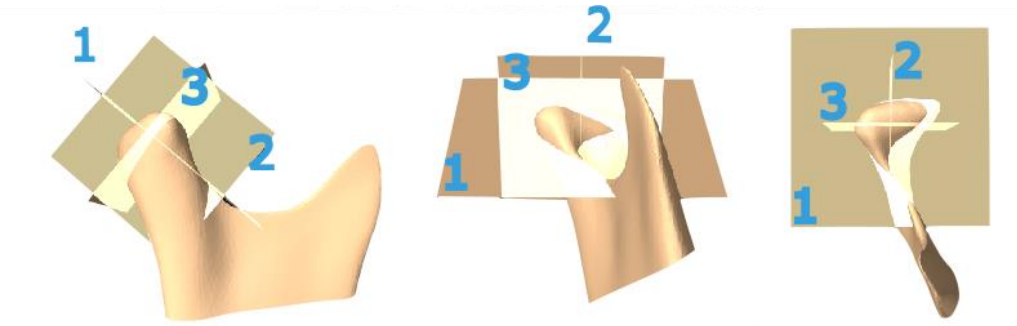

Figure 8: constraint set up for the temporomandibular joint (1: articular constraint; 2: lateral constraint; 3: posterior constraint) in side view, front view and top view respectively

Muscles were modeled as Hill-type actuators using properties found in literature [34][35]. A Hill-type muscle model describes a skeletal muscle as a one-dimensional combination of mechanical building blocks. Often this consists of a spring or inextensible cable for the tendon and a parallel combination of a spring and an active element, which mimics muscle activation and stretching [36]. The muscles included in the model are the temporalis, which was split into a posterior (PT), medial (MT) and anterior part (AT), the deep (DM) and superficial masseter (SM), the medial pterygoid (MP), the inferior (ILP) and superior head of the lateral pterygoid (SLP), the posterior (PM) and anterior mylohyoideus (AM), the anterior digastric (AD) and the geniohyoideus (GH).

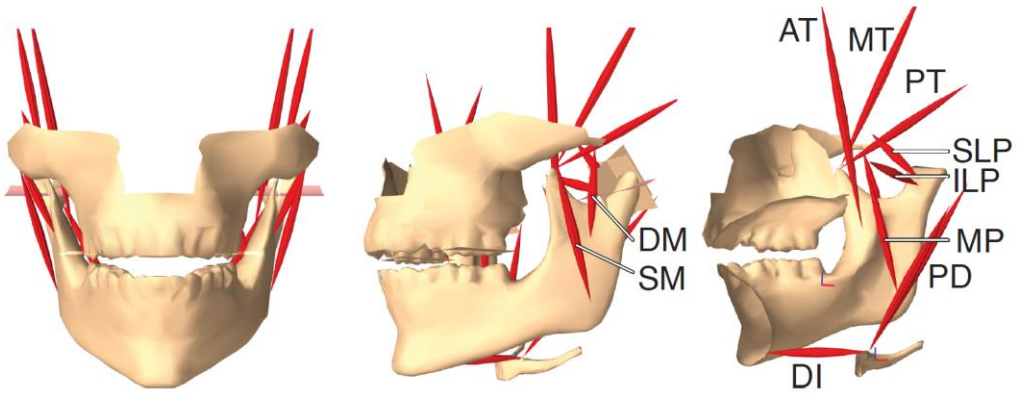

Figure 9: annotated muscles of the model (AM, PM, GH not shown)

Previously this model was used for forward dynamics investigations, for example of chewing [1], as well as for inverse dynamics simulations, for example to predict muscle activation patterns of hemimandibulectomy patients [11] and has generally shown good consensus with *in vivo* studies.

Regularization and Inverse Simulations

Since many simulations in this thesis are inverse dynamics simulations this chapter will give a short overview of the methods that are used to derive the optimal muscle activation pattern for our models. Mathematically speaking inverse simulations pose an optimization problem, since we are trying to find a muscle activation pattern, which yields a movement that is as close as possible to a predefined, desired trajectory. Due to the large number of muscles located around the human jaw, muscle redundancy can occur [33]. Muscle redundancy describes a state of the system where more than one muscle activation pattern would lead to the desired movement, for example we can pull the mandible by unilaterally activating a variety of muscles. This means we have to somehow define which muscle activation is “the best” for our simulation case.

Generally this is done by adding a regularization term which introduces an additional penalty for solutions that are not ideal [37][38]. Which kind solution is seen as ideal depends strongly on the regularization term. In this thesis all optimizations will try to minimize muscle activation, which tries to mimic the physiological concept of energy conservation. To find the optimal activation pattern we use L1- and L2-regularization terms.

L1-Regularization

A L1-regularization term is defined as [37][38]:

$$\|\boldsymbol{x}\|_1 = \sum_{i=1}^{n} |x_i| \qquad (1)$$

Here $\boldsymbol{x}$ denotes a vector containing the variables, e.g. muscle activation for all muscles and to compute the L1-norm we take the sum of the absolute values of all variables. Figure 10 shows the L1-regularization term for values between -100 and 100. This function increases linearly and hence tends to solely select the best suited muscle, which will be activated strongly while other muscles will be neglected, since their activation is strongly penalized.

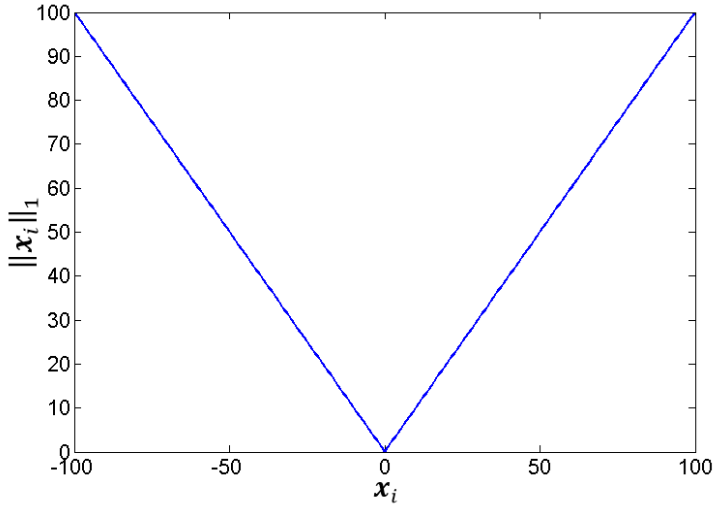

Figure 10: increase of L1-regularization term

In ArtiSynth we generally solve inverse simulations as a quadratic program (QP), which can lead to problems if we have a system with more variables than equations. For these cases the H-matrix (which will be explained in Chapter 3) is singular, but the L1-regularization term has no influence on the H-matrix [33]. In this case a L2-regulariaztion with a very small weight has to be added as well.

L2-Regularization

A L2-regularization term is defined as [37][38]:

$$\|\boldsymbol{x}\|_2^2 = \sum_{i=1}^{n} {x_i}^2 \qquad (2)$$

In this case we take the sum of squares of the values of all variables. Plotting the change of the norm with increasing values (figure 11) shows a convex function.

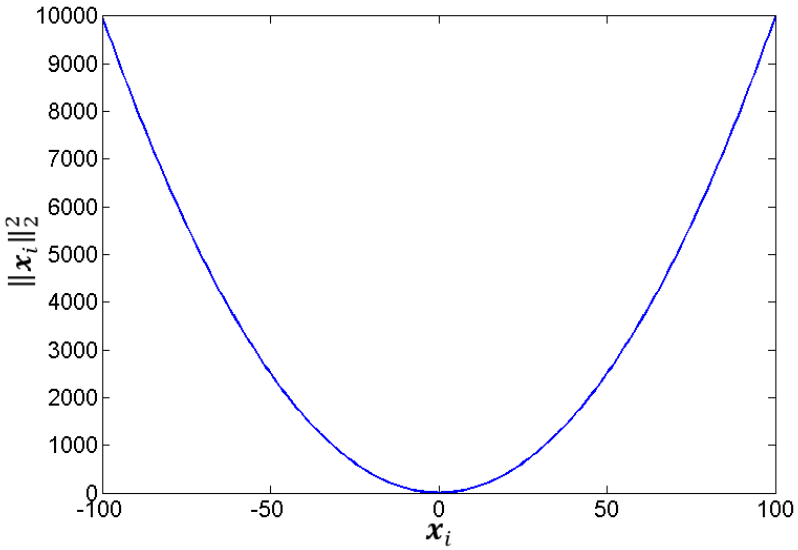

Figure 11: increase of L2-regularization term

This function tends to spread the muscle activation out over multiple muscles instead of strongly activating the one optimal muscle. This behavior occurs due to the fact that the L2-regularization term is slowly approaching its minimum and hence the penalty for activating muscles that are close to the optimal solutions is still quite small [38].

CHAPTER 3:
INVERSE SIMULATION WITH REACTION FORCE TARGET

Introduction

In this chapter, we present a new kind of inverse dynamics simulation that uses a reaction force goal as well as a movement goal for optimization. Existing inverse simulation tools only consider target movement, however many tasks require motion and applied forces. For example the biomechanical tasks of wiping on a surface or grinding your teeth cannot be accomplished by simply defining a movement trajectory. Such tasks need a second input variable that can be used to define the amount of force that has to be applied to the surface during the motion. Therefore we developed and evaluated a reaction force target for inverse dynamics simulations.

The most straight forward way of conducting a dynamic biomechanical study is to use a forward dynamics approach. Using this approach the input of a simulation consists of the activation levels of all muscles in the system. Using different properties of the muscles, e.g. maximum muscle force and optimal fiber length, the forces created by these muscles can be computed by solving the forward dynamics. Additionally, this approach computes constraint forces as well as the movement of the involved bodies.

The biggest drawback in using forward dynamics simulations, is the measurement of muscle activations, which are used as input for the simulation. The most common, noninvasive method for investigations of muscle activation is electromyography (EMG). Unfortunately, EMG is not an appropriate tool for the smaller muscles of the masticatory system, since it often struggles with the problems that occur due to the large number of muscles located in the small

jaw region [6]. The abundance of muscles makes the placement of EMG electrodes a complicated task and even with correctly placed electrodes, the problem of recording signals from multiple overlaying muscles stays unsolved. Furthermore, it is a very hard task to record EMG data for multiple muscles at the same time, without interference between the separate recordings.

As described above, a forward dynamics simulation method would require a trial-and-error approach to define the activation patterns for different movements, due to the lack of experimental data on muscle activation. To overcome this problem, an inverse dynamics simulation could be used. An inverse dynamics simulation uses a predefined output state to establish a set of input values that will make the simulation accomplish the predefined output state. Previous to this project, the inverse solver in ArtiSynth was only able to use a movement goal as input, which defined a movement trajectory for a body. Instead of using the muscle activations as an input, the simulation computes a muscle activation pattern that will yield the predefined movement trajectory. Afterwards this activation pattern is used to solve the forward dynamics to again compute muscle forces, constraint forces and the actual movement of the bodies.

Reaction forces can play an important role for biomechanical simulations, for example during running or chewing. Generally, reaction forces are experimentally measured, for example using force plates to measure ground-reaction forces during gait. These measured reaction forces are played back as external forces in a gait simulation [10]. However there are some systems where measuring reaction forces can be very tedious. For example, it is hardly possible to measure bite force without interfering with the system itself, since even a force transducer with a thickness of 1mm can alter one's ability to generate bite force comfortably [7].

Due to the problems presented above, we decided to incorporate reaction forces into the optimization of the inverse dynamics algorithm. This will enable the user to easily investigate the effects of different levels of reaction forces for systems where measuring them would be very challenging. Furthermore, a reaction force goal will lead to more stable simulations, since instead of simply applying reaction forces as external forces, they are now incorporated into the optimization process. In addition, our approach will offer the user more flexibility in the development of new models, because, using our approach, the user can decide if he wants to use a contact model or simply apply external forces for different parts of a model. To the best of the author's knowledge this is the first use of an inverse dynamic simulation using a dynamic movement as well as a reaction force goal simultaneously.

Methods

For this chapter we created a new Java class that contains the math to compute the reaction force target.

Inverse Dynamics Simulations

In general, simulations in ArtiSynth are governed by Newton's second law, in the form of [11][33]:

$$\boldsymbol{M\dot{u}} = \boldsymbol{f}(\boldsymbol{q},\boldsymbol{u},\boldsymbol{t}) = \boldsymbol{f}_{\boldsymbol{p}}(\boldsymbol{q},\boldsymbol{u}) + \boldsymbol{f}_{\boldsymbol{a}}(\boldsymbol{q},\boldsymbol{u},\boldsymbol{a}(\boldsymbol{t})) \quad (1)$$

where $\boldsymbol{q}$ denotes the position state vector, $\boldsymbol{u}$ denotes the velocity state vector, $\boldsymbol{a}$ denotes the muscle activation levels and $\boldsymbol{M}$ denotes the mass matrix. The forces are separated into a passive part $\boldsymbol{f}_{\boldsymbol{p}}$ (describing e.g. tendon forces) and an active part $\boldsymbol{f}_{\boldsymbol{a}}$. For controlling the inverse simulation we will describe the muscles by a Hill-type model:

$$\boldsymbol{f}_{\boldsymbol{a}} = \boldsymbol{\Lambda}(\boldsymbol{q},\boldsymbol{u})\boldsymbol{a} \quad (2)$$

In equation (2) $\boldsymbol{\Lambda}$ denotes a matrix that is dependent on the position and velocity state vectors. To solve the equation, ArtiSynth assumes that $\boldsymbol{f}_a$ is locally linear with respect to $\boldsymbol{a}$.

Currently, the inverse solver is only supporting bilateral constraints $\boldsymbol{G}(\boldsymbol{x})$, where $\boldsymbol{x}$ is the position of the body. These constraints are invoked by forces onto $\boldsymbol{G}^T(\boldsymbol{x})$. This leads to a new formulation of (1):

$$\boldsymbol{M\dot{u}} = \boldsymbol{f}_p(\boldsymbol{q},\boldsymbol{u}) + \boldsymbol{f}_a\big(\boldsymbol{q},\boldsymbol{u},\boldsymbol{a}(\boldsymbol{t})\big) + \boldsymbol{G}^T(\boldsymbol{x})\boldsymbol{\lambda} \qquad (3)$$

The Lagrange multipliers $\boldsymbol{\lambda}$ contain the constraint force magnitudes. To solve (3) we have to integrate forward in time. This is done using a first-order integrator, which is semi-implicit with respect to the passive forces $\boldsymbol{f}_p$. After introducing a time step h and a superscript i, to denote the time point, we get:

$$\boldsymbol{Mu}^{i+1} = \boldsymbol{Mu}^i + \boldsymbol{hf}_p^{i+1}(\boldsymbol{q},\boldsymbol{u}) + \boldsymbol{h\Lambda}^i(\boldsymbol{q},\boldsymbol{u})\boldsymbol{a} + \boldsymbol{G}^{iT}(\boldsymbol{x})\boldsymbol{\lambda} \qquad (4)$$

To approximate $\boldsymbol{f}_p^{i+1}$ we use:

$$\boldsymbol{hf}_p^{i+1} \approx \boldsymbol{f}_p^i + \frac{\boldsymbol{\partial f}_p}{\boldsymbol{\partial x}}\Delta\boldsymbol{x} + \frac{\boldsymbol{\partial f}_p}{\boldsymbol{\partial u}}\Delta\boldsymbol{u} \qquad (5)$$

$$= \boldsymbol{f}_p^i + \frac{\partial f_p}{\partial x} h u^{i+1} + \frac{\partial f_p}{\partial u}(u^{i+1} - u^i)$$

Combining this with (4) and using the acceleration constraint $g^i = -h\dot{G}^i u^i g^i = -\boldsymbol{h}\dot{\boldsymbol{G}}^i u^i$ leads to:

$$\begin{pmatrix} \widehat{\boldsymbol{M}} & -\boldsymbol{G}^T \\ \boldsymbol{G} & 0 \end{pmatrix}\begin{pmatrix} u^{i+1} \\ \lambda \end{pmatrix} = \begin{pmatrix} \boldsymbol{Mu}^i + h\widehat{\boldsymbol{f}_p} + h\boldsymbol{\Lambda a} \\ \boldsymbol{g}^i \end{pmatrix} \qquad (6)$$

with

$$\widehat{\boldsymbol{M}} \equiv (\boldsymbol{M} - h\frac{\boldsymbol{\partial f}_p}{\boldsymbol{\partial u}} - h^2\frac{\boldsymbol{\partial f}_p}{\boldsymbol{\partial x}}),\ \widehat{\boldsymbol{f}_p} \equiv \boldsymbol{f}_p^i - \frac{\boldsymbol{\partial f}_p}{\boldsymbol{\partial u}}\boldsymbol{u}^i$$

This gives us $\boldsymbol{u}^{i+1}$ and $\boldsymbol{\lambda}$, which now describes the magnitude of the constraint impulses, for a specific muscle activation pattern. We can now define a target velocity trajectory $\boldsymbol{v}^*$ in a

target velocity space $\boldsymbol{v}$. The target velocity space and the velocity space are connected by the Jacobian matrix $\boldsymbol{J_m}$ via $\boldsymbol{v = J_m u}$. Furthermore (6) shows that

$$\boldsymbol{u^{i+1} = u_0 + H_u a}, \qquad (7)$$

where $\boldsymbol{u_0}$ is the solution for zero muscle activations and the columns of $\boldsymbol{H_u}$ give the solution for (6) with a right hand side of

$$\binom{\Delta e_j}{0},\ \boldsymbol{e_j \equiv elementary\ unit\ vector}. \qquad (8)$$

We now try to minimize the error $\left\|\boldsymbol{u^* - J_m u^{i+1}}\right\|$, which can be written using $\boldsymbol{a}$:

$$\boldsymbol{\Phi_m(a) = \frac{1}{2}\|\bar{v} - H_m a\|^2} \qquad (9)$$
$$\boldsymbol{\bar{v} \equiv v^* - J_m u_0} \quad \text{and} \quad \boldsymbol{H_m \equiv J_m H_u}.$$

Inverse Dynamics Simulation using Reaction Force Targets

To enable the simulation to use the constraint force magnitudes for optimization we saved $\boldsymbol{\lambda}$ and used it to create an implementation of a force target, mathematically similar to the movement target described above.

For that purpose, we define constraint force goals $\boldsymbol{\xi}$, which are connected to the constraint impulse magnitudes $\boldsymbol{\lambda}$ by $\boldsymbol{h\xi = J_c \lambda}$, where $\boldsymbol{J_c}$ is again a connecting Jacobian. Using the same approach as above we receive the optimization term:

$$\boldsymbol{\Phi_c(a) = \frac{1}{2}\left\|\bar{\lambda} - H_c a\right\|^2} \qquad (10)$$

$$\boldsymbol{\bar{\lambda} \equiv h\xi - J_m \lambda_0} \quad \text{and} \quad \boldsymbol{H_c \equiv J_c H_\lambda}$$

Since $\boldsymbol{u^{i+1}}$ is computed simultaneously with $\boldsymbol{\lambda}$, we can use both movement and force goals at the same time.

It is likely that the same movement can be achieved by different muscle activation patterns, due to the sheer number of jaw muscles. To receive a consistent activation pattern we include a weighted l^2 - norm regularization term, $\frac{1}{2}\boldsymbol{a}^T\boldsymbol{W}\boldsymbol{a}$, using a diagonal weighting matrix $\boldsymbol{W}$.

If we now combine the movement target and the force target optimization terms with the regularization term, we get the final quadratic term:

$$\min_{a} \quad w_m \Phi_m(a) + w_c \Phi_c(a) + \frac{w_a}{2} a^T W^{-1} a \qquad (11)$$
$$with\ 0 \leq a \leq 1$$

where w_m, w_c and w_a are weight terms to adjust the importance of the different cost terms.

Toy Model

To verify the reaction force target, we created a simple toy model. This test case consists of a small rigid body, a planar constraint and six muscles that are attached to the body with force vectors in x-, y-, z- directions and the respective negative directions. These muscles will be used to create a simple movement pattern.

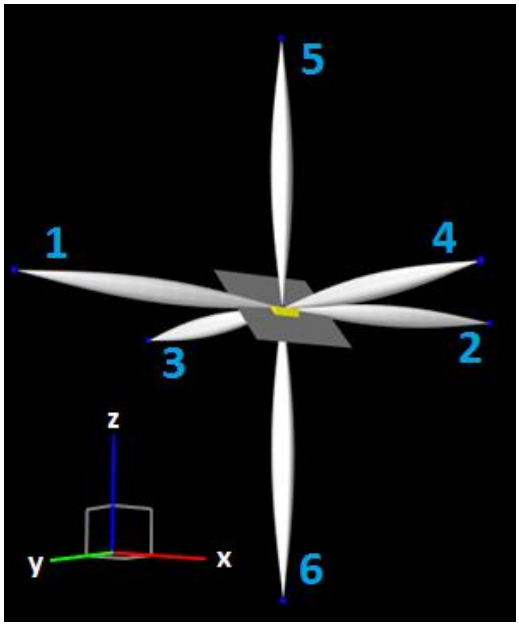

Figure 12: toy model consisting of 6 muscles, one rigid body and a planar constraint

By adding a movement as well as a reaction force goal, this model can be used to verify the general correctness of our reaction force goal implementation. Furthermore we can check if the interaction of the different cost terms yields the desired result. Figure 12 shows the set-up of the toy model. We ran simulations using a movement goal that increases the y- and z- coordinate by 50 cm to create an upwards movement of the body along the constraint. At the same time, a reaction force goal of 50 N was applied. The muscles in this simulation are modeled using ArtiSynth's *SimpleAxialMuscleModel* [33]. All muscles were initialized with a maximal force of 40N, a damping coefficient of 0.1 N*m/s and a stiffness of 0 N/m.

Upper Extremity Model

To show our approach in a biomechanical setting we adapted the upper extremity model created by Saul et al. [39]. We added a planar constraint to the hand of the model, which makes the model act like it is holding a handle.

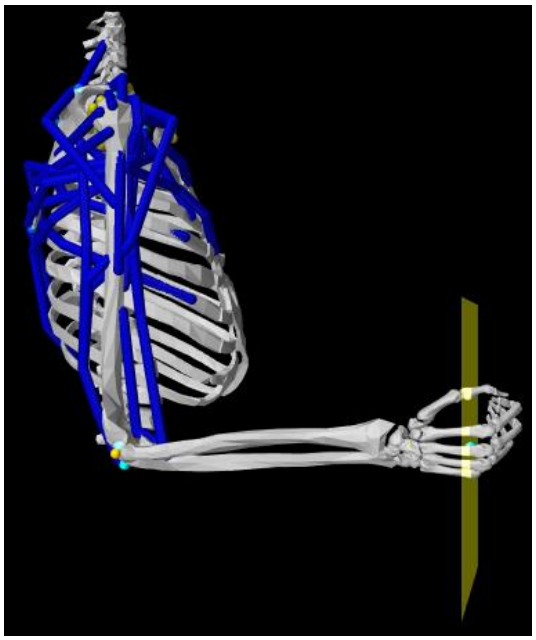

Figure 13: adapted upper extremity model

By adding a reaction force target to the simulation, we can now make the model pull and push on the handle. This isometric force task is solely controlled by the force target itself, since the movement goal is kept static at the initial position. Figure 13 shows the adapted model.

Moreover, we created a simulation using the adapted model with a force target of 10N to show the increase in stability due to the use of the reaction force target. The results of this simulation will be compared to another simulation using the original model, where we applied 10N as an external force.

Results

Toy Model

The toy model moved 50 cm in z- and y- direction, while simultaneously creating a constraint force of 50N.

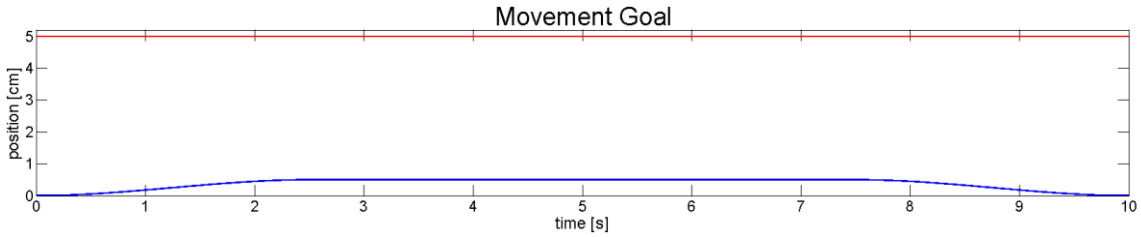

Figure 14: Input movement trajectory for toy simulation (red: x- axis, blue: y- and z- axis)

To achieve the movement as well as the constraint force, two muscles are activated. Muscle 3 is activated with 96% and muscle 6 with 78.1%. Figure 15 shows the simulation at t=0s and t=5s, which denotes maximum displacement and maximum force. Figure 16 shows the muscle activation pattern as well as the constraint reaction force over time. The simulation achieved the target motion as well as the target reaction force.

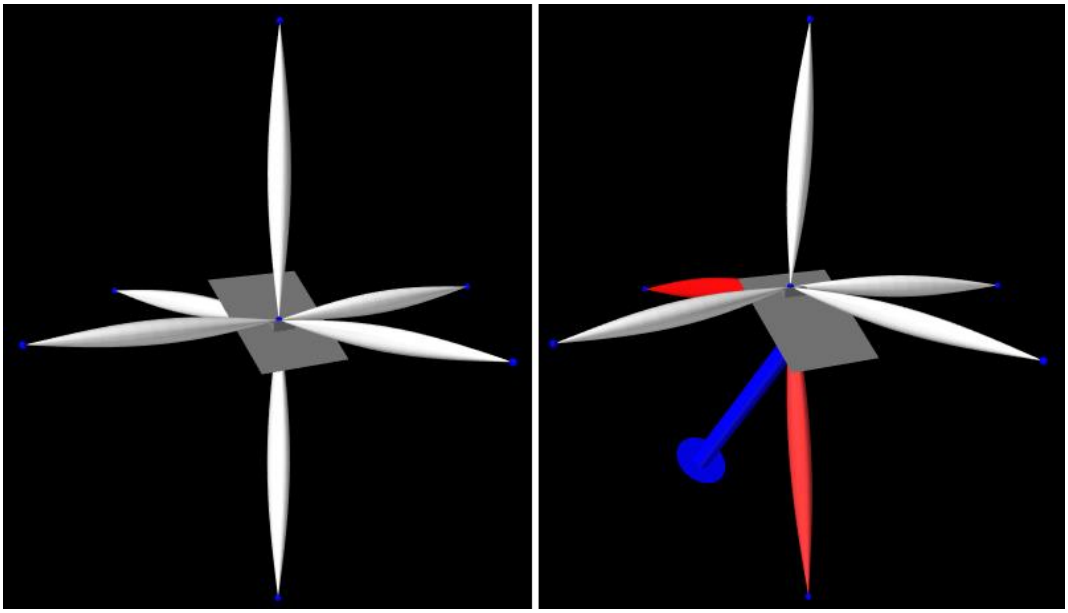

Figure 15: toy model in original state, compared to state with 50N force goal and fulfilled movement goal (red muscles are activated, blue arrow is representing reaction force)

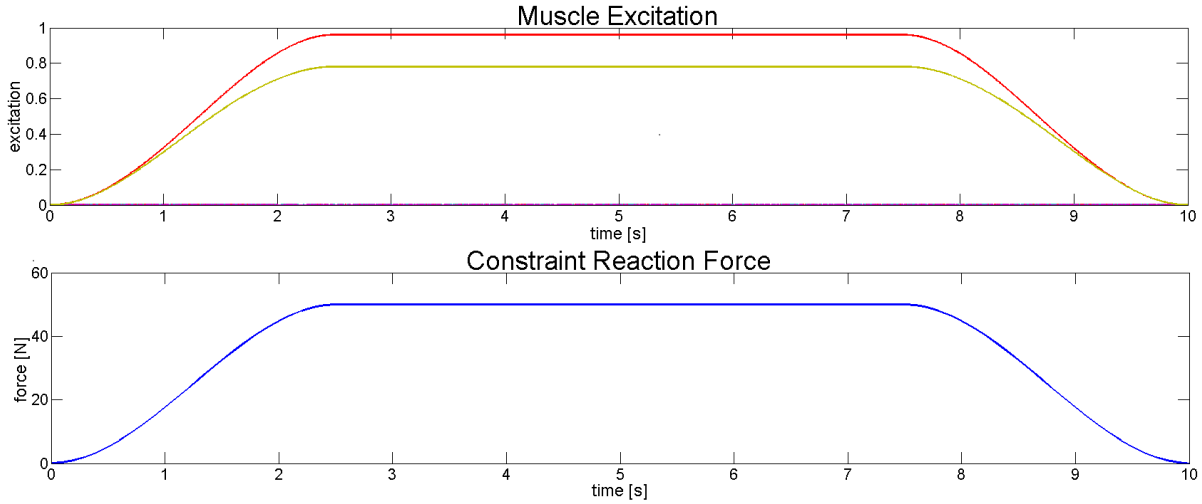

Figure 16: muscle activation pattern (red: muscle 3, brown: muscle 6); constraint reaction force over time

Upper Extremity Model

The simulation with a reaction force target creates a constraint normal force of 9.86N. The only movement is a slight rotation of the elbow at the beginning of the simulation (figure 17). The highest activations are created in the deltoid3 with 81.6%, the latissimus dorsi2 with 35% and the latissimus dorsi3 with 32.3%.

Using an external force of 10N produces a simulation with a completely misplaced arm. For external forces higher than 6N, the arm starts moving inwards and folds in around 6.5N. A visual comparison of the results for different force levels in each model can be found in figure 17.

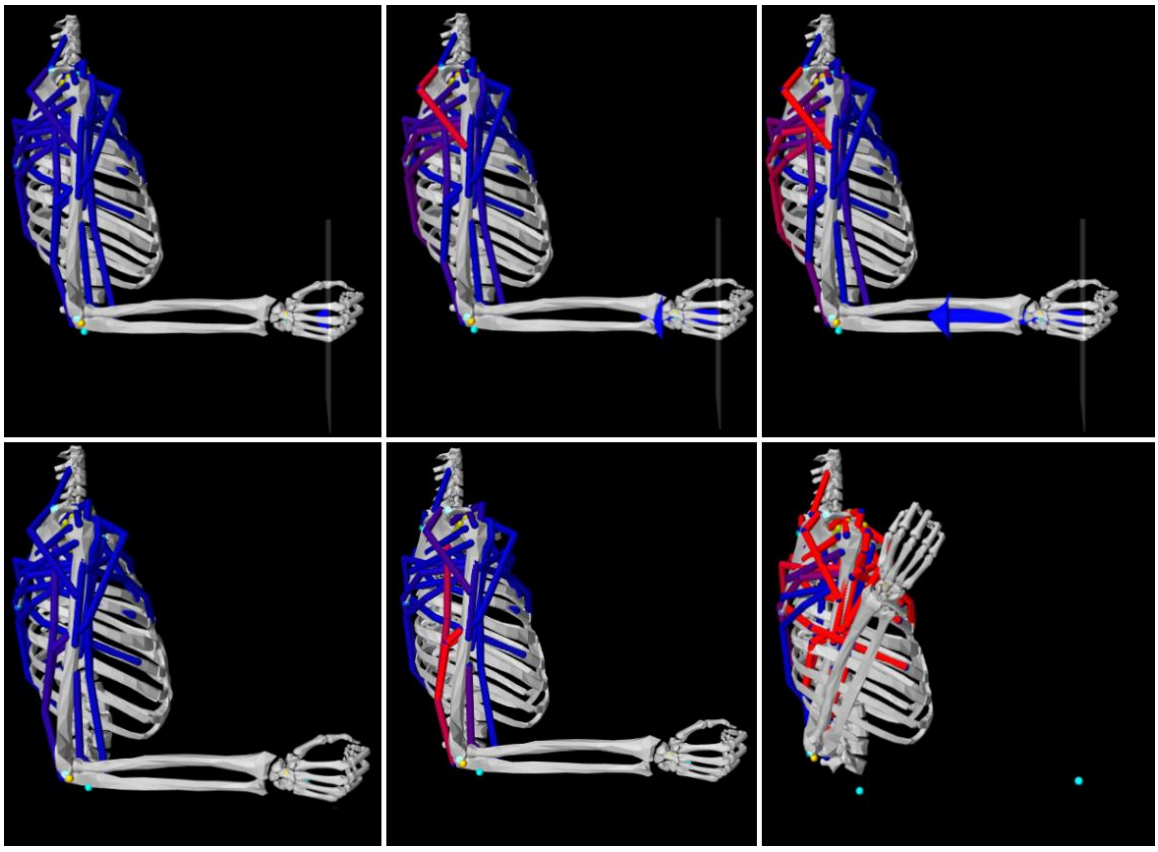

Figure 17: results for 1N, 5N and 10N; upper three images: adapted model with reaction force goal; lower three images: original model with external force

Discussion

This chapter presents a new quadratic optimization term that enables the inverse solver in ArtiSynth to use reaction force goals in addition to movement goals. This provides users with more flexibility in the development of new models and should give more realistic results for simulations that need a substantial amount of force that is not primarily used for movement itself.

To validate the implementation of the reaction force goal, we created a series of simple simulations.

Toy Model

The results of the test case show that our implementation of a reaction force goal works correctly. The model is able to create the predefined amount of constraint normal force, while still following the movement goal. Muscles 3 and 6 are activated, because their combination leads to the muscle force vector that is most suited to create normal force on the constraint. Furthermore, muscle 3 is activated stronger. This enables the body to slide upwards along the constraint, in accordance to the movement goal.

Overall, this simple test case shows that our implementation of the reaction force goal works properly. To our knowledge, this is the first example of the use of a movement and reaction force goal simultaneously.

Upper Extremity Model

It should be stated that the maximal muscle forces of the model are somewhat arbitrary, since we were not interested in achieving physiological force levels. For this study the upper extremity model was used to test how our approach works in the context of an anatomical system and since the same muscle properties were used for both approaches this should be sufficient for a comparison study. The upper extremity simulations show that our approach, using a reaction force goal, leads to more stable simulations, since we were not able to create a properly working simulation with an external force of 10N. Also, figure 17 shows that the external force simulation leads to a quite different activation pattern compared to our approach for a force of 5N. In general, the muscle activations of the external force simulation seem to be slightly higher

than the excitations of the muscles using a reaction force target. The results showed that our approach yields superior results, especially for tasks that require high forces, since we were able to produce even higher constraint reaction forces than the presented 10N using the force target, while the model with an applied external force stops working correctly at around 6.5N.

CHAPTER 4:
INVERSE DYNAMICS SIMULATION OF SLEEP BRUXISM

Introduction

Sleep bruxism (SB) is a sleep-related movement disorder, which is characterized by unconscious tooth grinding and clenching [24]. Bruxism can lead to severe abrasion of the tooth crowns as well as to serious temporomandibular joint problems, which can make everyday tasks like speech and mastication tedious and painful. The occurrence of bruxism is considered to be strongly linked to a stressful lifestyle [5]. In the last decades the connection between stress and bruxism has led to an increase in occurrence of bruxism and therefore to an increased importance of the understanding of sleep bruxism.

Our ability to investigate the mechanisms that underlie bruxism, such as the role of different jaw muscles during bruxism, is limited by ethical and patient safety restrictions. The use of noninvasive measures, like EMG, is only suitable for the bigger jaw muscle and not for recording data for the smaller muscles of the system, as discussed earlier in this thesis. To solve this problem we created an inverse dynamics biomechanical simulation of bruxism. An inverse simulation uses a defined output to compute the activations needed to yield the predefined end state. We developed this simulation using the open source biomechanics simulation toolkit ArtiSynth [33].

Since bruxism is characterized by a movement with an accompanying clenching force we drive our simulation using a movement and a force goal at the same time. This will enable us to

mimic the bruxing conditions as realistically as possible. For our simulation we defined different simple grinding patterns that most likely occur during bruxism.

Often friction can be neglected in jaw muscle simulations, since saliva acts as a lubricant, but due to the huge closing forces present during sleep bruxism, friction could play an important role. Douglas et al. investigated the frictional effects between teeth using an artificial mouth [40]. Furthermore Zheng et al. investigated the change of the friction coefficient over an increased number of grinding events [41][42]. They conclude that the friction coefficient of healthy teeth of non-bruxers is around 0.1, but can drastically increase with wear. Currently there is no friction model for bilateral constraints available in ArtiSynth, hence we implemented a static friction model for bilateral constraints.

To validate our predictions, the computed activation patterns will be compared with EMG recordings. Unfortunately, we were only able to gather isolated EMG recordings for the larger jaw muscles (e.g.: masseter, temporalis), due to the limitations of EMG recording of the facial region described before. Lavigne et al. published EMG data of a polysomnographic recording in a sleep lab [29]. They report differential activation of the left and right temporalis muscle with magnitudes switching at every bruxism event. Furthermore they report bilateral activation of the masseter with higher activation on the working side. They also report co-activation of the submental muscles during bruxism.

Methods

For the development of this project we created a new Java class in the ArtiSynth project which contains our adapted model and includes all input and output probes to set and record movement trajectories as well as bite force goals. Moreover another class was created that computes the static friction and applies an external frictional force to the model.

Model Set-Up

The model developed for this project was based on a previously published model by Hannam et al. [1]. This model contains:

- posterior, medial and anterior temporalis (PT, MT, LT)
- deep and superficial masseter (DM, SM)
- medial pterygoid (MP)
- inferior and superior head of the lateral pterygoid (IP, SP)
- posterior and anterior mylohyoideus (PM, AM)
- anterior digastric (AG)
- geniohyoideus (GH)

All muscles are present on both sides of the mandible.

To model the temporomandibular joint, three bilateral constraints were used on the working side of the model, constraining lateral, posterior movement as well as movement against the articular surface, hence this set up only allows for rotation of the left condyle. On the non-working side, the joint was modeled using one bilateral constraint, enabling the condyle to move freely on an angled plane.

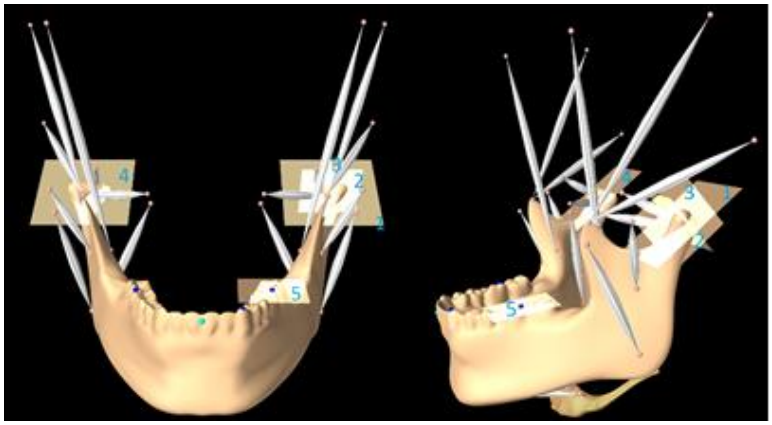

Figure 18: model setup - 1: left articular fossa constraint, 2: left posterior constraint, 3: left lateral constraint, 4: right articular fossa constraint, 5: bite constraint

We found conflicting EMG studies suggesting different behavior of the masseter [29][43]. One group shows equal activations on both sides, while another study suggests higher activation on the working side. For this thesis, we only investigated the second version, using higher activations on the working side during bruxing events. For this purpose, we added a precondition to our model that only allows all four heads of the masseter to be activated simultaneously and enforces an activation twice as high on the left masseter, which is the working side of our model, compared to the activation of the two heads on the right side.

Furthermore, an additional planar constraint was added at the first left molar or first left canine respectively. This constraint was simulating tooth contact during grinding and clenching and was used as well to define the closing force goal.

Friction for Bilateral Constraint

ArtiSynth only contains a friction model for unilateral constraints [33]. A unilateral constraint allows the constrained body to move off the constraint in one direction, but prohibits it from penetrating it. Unfortunately, the inverse solver only supports bilateral constraints, which prohibit the body from moving off the constraint in any direction. For most jaw movements, this neglect of friction would have been justified due to the friction-reducing effect of the saliva, but because of the huge closing forces that are applied during the clenching behavior associated with bruxism, frictional effects could have a relevant impact on the results of our simulation. Therefore we created a friction model to investigate the effects of friction on the bruxism simulation.

We implemented a static friction model:

$$\boldsymbol{F}_f = -k\|\boldsymbol{F}_n\|\frac{\boldsymbol{v}}{\|\boldsymbol{v}\|} \qquad (1)$$

where $\boldsymbol{F}_n$ represents the normal force of the surface, $\boldsymbol{v}$ represents the velocity of the body (which is always in the plane of the bilateral constraint) and k defines the coefficient of friction. $\boldsymbol{F}_f$ is applied at the bite point and acts in the negative direction of velocity.

Simulations

We simulated two different grinding patterns:

- outwards grinding from ICP to a left lateral canine edge-to-edge contact position
- inwards grinding to ICP from a left lateral canine edge-to-edge contact position

A movement target for the lower incisor point was added to input the movement patterns. For both patterns, we added a force goal for the constraint on the left first molar or the left canine, to simulate bite force. Trajectories for the movement as well as the force target were created using cubic splines. The duration of the simulation is 0.7 seconds, after an initiation phase of 0.3 seconds to isolate motion and bite force creation. The bite force goal was set to 200N for the simulations with a bite constraint on the first molar. A force goal of 150N on the canine constraint was used for the outwards movement, since applying force on this more protruded position requires higher muscle activations.

Furthermore, a force goal was added to the posterior constraint of the left condyle. This had to be done due to the fact that the posterior constraint is bilateral and it could prevent an anterior movement, even though protrusion of the mandible is a normal movement. Hence this second force target was used to ensure that the computed muscle activation pattern will yield the desired movement without negative activation of the posterior constraint. Values for all posterior constraint force goals can be found in table 1. The force goal for the outwards simulations was increased over the course of the simulation to mimic forces that would press the condyle against

the back wall of the articular surface during the outwards translation of the mandible. For both outwards simulations, a second version with a constant force goal was created to investigate the influence the posterior force of the temporomandibular joint on the muscle activation pattern. For the inwards grinding simulations, the force goal on the posterior constraint was chosen to ensure a positive, but small force on the posterior constraint.

Table 1: reaction force goals for different simulation settings

		Molar	Canine
Outwards	high	30N to 110N	30N to 82.5N
	low	constant 30N	constant 30N
Inwards		45N to 20N	50N to 26.2N

Results

Outwards Grinding on Molar

Increasing Posterior Constraint Force

Figure 16a shows the muscle activation pattern predicted for an outwards grinding movement to a left lateral position. For this case, we get high activations in both heads of the masseter on the working side that start at 87% and decrease to 65%. Furthermore, activation of all three parts of the working side temporalis muscle increases over time, with the strongest activation in the anterior part (80%). The posterior part of the contralateral mylohyoid muscle is also activated strongly, with a maximum of 68%. Additionally the two heads of the non-working side lateral pterygoid muscle are activated, with a higher activation of the inferior head, while there is only little activation of the right lateral pterygoid.

The constraint forces for this simulation can be seen in figure 20 and figure 21. Bite force starts at 203N and decreases to 196N. The posterior constraint force starts at 0N at goes up to 74N.

Constant Posterior Constraint Force

In comparison to the first case, we see an increased level of activation for both heads of the masseter, the posterior part of the contralateral mylohyoid and both heads of the lateral pterygoid on both sides, while all three parts of the working side temporalis have a decreased activation. Interestingly, the posterior part of the working side temporalis muscle is not used at all in the second half of this simulation. Using the lower posterior constraint force goal the constraint force is 0 at the beginning and decreases to -7.5N at the end of the simulation.

Inwards Grinding on Molar

Another simulation was created using the bite constraint on the first molar and the inwards movement goal. Again we see high activation of the masseter on the working side (63%) that decreases slightly over time (59%). The activation in all three parts of the left temporalis is decreasing over time, while the activation of the right temporalis increases. At the end of the movement activations of all parts of the right side temporalis are higher than their respective parts on the left side. Also, bilateral activation of the medial pterygoid muscle occurs during this simulation.

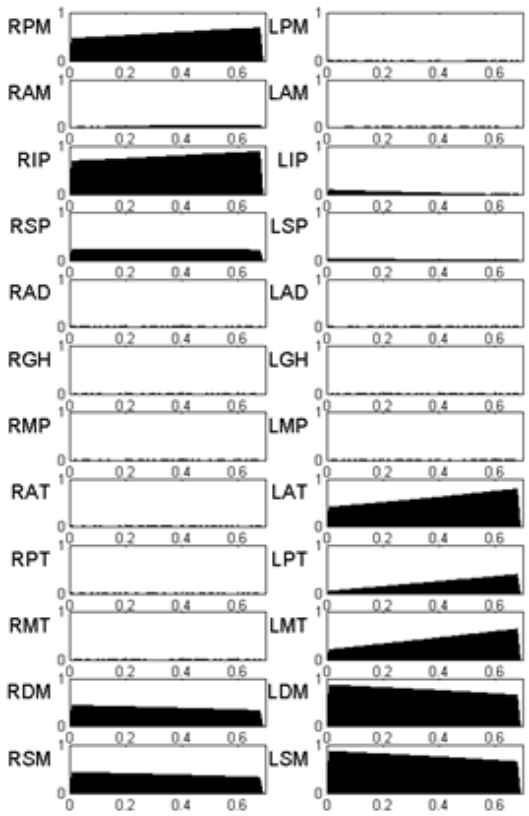

Figure 16a: muscle activation pattern for outwards grinding on first molar

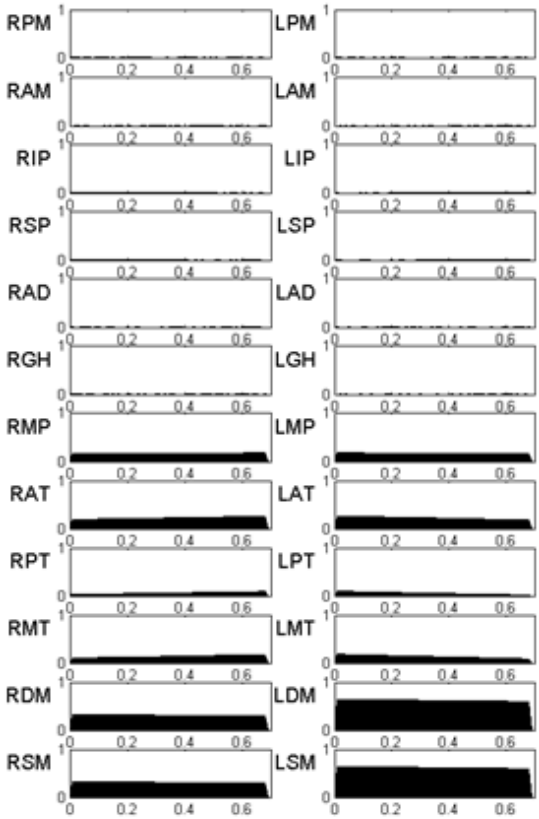

Figure 16b: muscle activation pattern for inwards grinding on first molar

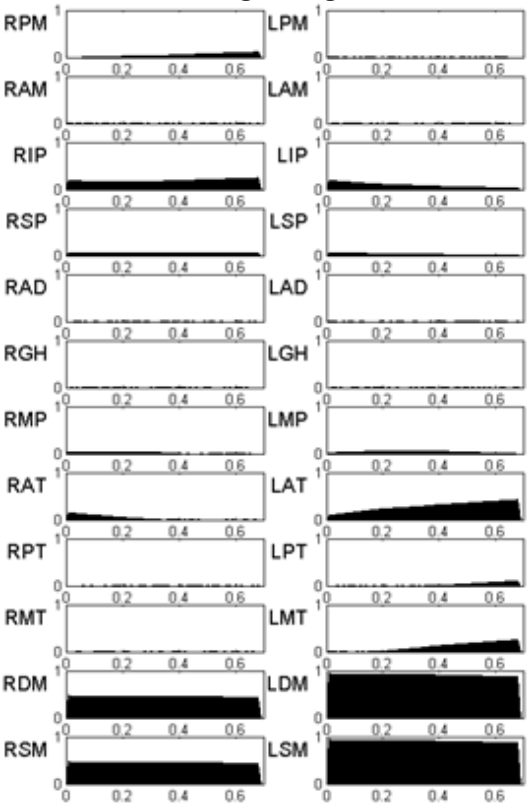

Figure 16c: muscle activation pattern for outwards grinding on canine

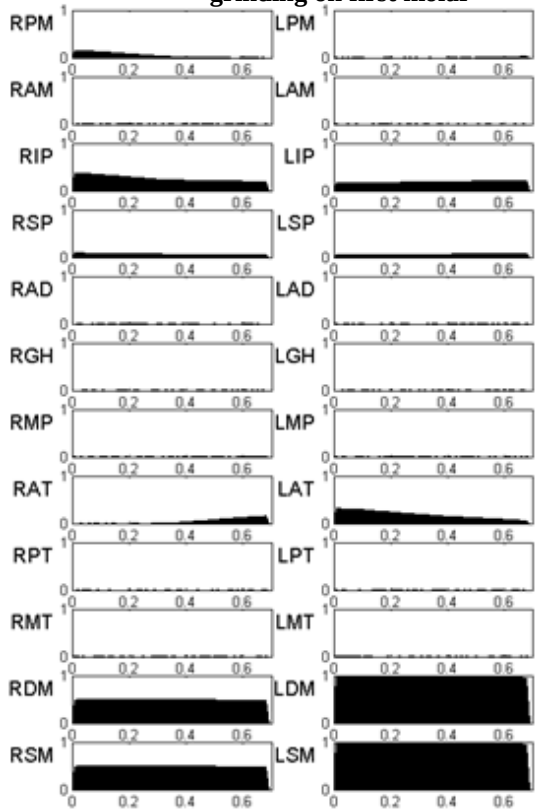

Figure 16d: muscle activation pattern for inwards grinding on canine

Outwards Grinding on Canine

For the first case, with an increasing posterior constraint force goal, the simulation predicts high activation of the left masseter, starting at 94% and decreasing to 87%. We also report increasing activation of the left temporalis, with the strongest activation in the anterior right temporalis. The right and the left inferior head of the lateral pterygoid start with a comparable activation level. While the right side muscle's activation is increasing over time, the left side muscle's decreases. The same trend occurs for the activation of the superior part of the lateral pterygoid.

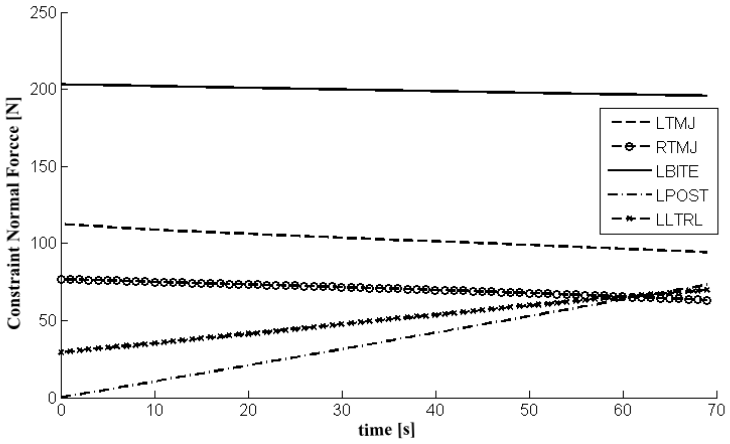

Figure 20: constraint forces with increasing posterior constraint goal

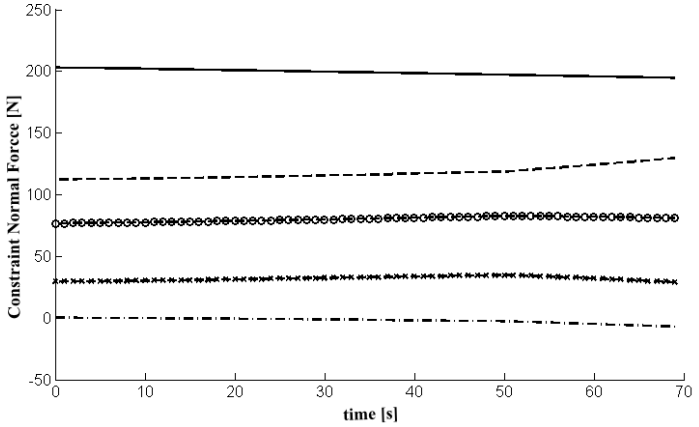

Figure 21: constraint forces with constant posterior constraint goal

Inwards Grinding on Canine

Again the highest activation occurs in the left masseter with an activation of 100%. For the temporalis, we only get bilateral activation of the anterior part, which decreases on the left side and increases on the right. Furthermore, bilateral activation of both heads of the lateral pterygoid occurs, with decreasing activation of the right inferior head and increasing activation of the left inferior head. There is also some activation of the posterior part of the right mylohyoid muscle for the first half of the simulation.

Discussion

The simulation results show that our new version of the inverse solver is able to recruit a muscle combination that will fulfill movement and bite force targets at the same time. This is not only important in the dental context presented in this study, but could also be used for various other tasks of the human body that include forces that are not solely used for movement.

Our investigations of the different movement patterns suggest that the masseter is the muscle mostly concerned with the creation of bite force. One reason for this is most likely our precondition of only allowing bilateral activation of the masseter. On the other hand, the muscle is also strongly activated for all inwards movements, even though the stronger activation of the left masseter is counteracting the direction of movement for these simulations. This suggests that the reason for its recruitment is the muscle vector of the masseter, which is nearly perpendicular to the bite plane and seems to be best suited for the creation of bite force.

To investigate the effects of friction during bruxism, we developed a static friction model for bilateral constraints. Even though static friction is a fairly simple representation, it is reasonable to use it in the context of our study, since we are looking at simple, continuous movements, with teeth contact at all times. We found conflicting values for the friction

coefficient of teeth, especially depending on the wear level of the teeth. We chose a friction coefficient of 0.3, which corresponds to a tooth surface that already experienced some wear, due to grinding, but is not yet worn drastically [40][41][42].

Our friction model is not directly incorporated into the system matrix of the inverse solver, hence it is applied after the optimal muscle activation pattern for the next time step is computed. Depending on the chosen time step and friction coefficient, this can lead to oscillations in the muscle activation patterns. Nevertheless, the same trend of muscle activation patterns occurs for these simulations. To solve this problem, we would need to incorporate unilateral constraints into the inverse solver, since friction is generally modeled as a unilateral constraint.

The changes in the activation pattern between the outwards grinding simulations on the first molar, using different posterior constraint forces, can be explained by looking at the different muscle force vectors. By using the posterior head of the left temporalis muscle, the simulation can increase the load on the posterior constraint of the temporomandibular joint, while creating additional bite force. On the other hand, creating bite force while keeping the constraint load small means that the masseter has to be activated more strongly, while particularly the posterior and medial head of the temporalis have to be activated less, because their force vectors are not only pulling upwards but backwards as well. Due to our precondition of activating both sides of the masseter, using a fixed ratio (0.5:1; right: left), we have to increase the activation of the right lateral pterygoid and posterior mylohyoid to pull the condyle downwards against the increased closing force. Additionally activation of the left lateral pterygoid occurs to reduce the force on the posterior constraint of the left condyle.

To compare the influence of the grinding position, we created a first molar simulation using the same outwards movement goal and a bite force goal of 150N, as used for the canine simulations. In the two cases, there are only slight differences in the activation of the temporalis and masseter. The main difference is the strongly reduced activation of the posterior part of the right mylohyoid and the right lateral pterygoid. Furthermore, a bilateral activation of the medial pterygoid occurs, with the activations of the right side diminishing over time. These increased activations are most likely used to create the posterior force instead of the lateral pterygoid and mylohyoid muscle.

Also, the force on the left TMJ constraint suggests that grinding at this anterior position will create high loads on the temporomandibular joints, since most closing muscles are better suited to create bite force around the molar region.

The role of the mylohyoid muscle in these simulations would need some further investigations. In general, the mylohyoid is not seen as a muscle of mastication, but if the hyoid is fixated, due to co-contraction of supra- and infrahyoid muscles, the mylohyoid could be used to pull the mandible inwards. Nevertheless the isometric force of this muscle is quite small, which means that even high activations would not necessarily have a major contribution to the movement of the mandible. Additionally, most EMG experiments record from all submental muscles with a single electrode and EMG channel, which makes the investigation of the role of the mylohyoid even harder.

For the inwards movement, the simulation predicts a more symmetrical muscle activation pattern. The activation of the left masseter will again be used to create the desired bite force. The left temporalis muscle decreases over time which is, to some extent, done to fulfill the small force target of the posterior constraint. Another reason for the decrease could be that once the

mandible comes closer to ICP, the masseter and medial pterygoid are better suited to create bite force.

The activation of the right temporalis is used to pull the mandible inwards. For this case, all muscle activation levels are significantly smaller than for the muscles activated during the outwards movement.

Comparing these results to the inwards grinding on the canine, we see an increased level of activation for the masseter, most likely again to create the bite force. Furthermore, the activation of the temporalis and medial pterygoid muscles vanishes, except for the anterior part of the temporalis muscle, which has the best force vector to create bite force without a posterior force component, of all temporalis parts. Since the medial and posterior part of the temporalis, on the respective side, were used to either control the movement of the molar simulation or control the force on the posterior constraint, the canine simulation has to activate additional muscles for the movement as well as the posterior constraint force. The simulation uses a bilateral activation of the lateral pterygoid and activation of the non-working side posterior part of the mylohyoid for this purpose.

In literature there are reports of a co-activation of the submental muscles during bruxism [29][43]. This is most likely to stiffen up the system using antagonistic co-activation [44]. Since we are not using a stiffness goal for our optimization and included a L2 regularization, this co-activation will not occur in our study, but due to the fact that this co-activation is not necessarily used for grinding nor clenching itself it is a reasonable assumption that including a stiffness goal would most likely increase the levels of activations, but would not necessarily change the pattern itself, except for the submental muscles. This is something that would be interesting to investigate in a future study.

Another limitation of our study is that the current implementation of the inverse solver only uses bilateral constraints, which means that the teeth in the simulation will always be in contact. Furthermore, it is impossible to model a joint, as complex as the temporomandibular joint, correctly using only bilateral constraints. The representation used in this paper only allows for rotation of the left condyle and free translation on an angled plane, modeling the articular surface, for the right condyle. This represents the most important degrees of freedom of the mandible during a lateral movement.

The fact that the simulation could choose an activation pattern that would lead to a negative force on the posterior constraint is a problem, since this would mean that the muscle pattern would actually lead to a protrusion of the condyle, which is a feasible movement that is only restricted by the bilateral constraint. We prevent this by using a second force goal on the posterior constraint, which made sure that during the whole simulation the overall muscle force could never have an anterior component.

The use of planar constraints is also a limitation of this study. A planar bite constraint represents flat teeth, which is not the normal case, but can be a consequence of bruxism in severe cases. While using constraint normal forces as optimization goals it is not possible to use bite constraints that are strongly angled, since the main force component of a constraint with a large angle would point inwards instead of upwards. This would mean that the bite force would be reduced drastically, since the closing muscles are no longer acting in the main direction of the normal vector of the constraint.

CHAPTER 5:
A DETAILED LATERAL PTERYGOID MODEL

Introduction

The lateral pterygoid is a small, but complex, muscle of mastication that is usually divided into two parts: the superior and inferior heads. Recent anatomical and EMG studies have found that the lateral pterygoid muscle (LPT) has a complex internal architecture, which could have important biomechanical consequences for TMJ loading [14]. Existing biomechanical jaw models do not account for the different LPT compartments; therefore, we developed a new detailed model of the LPT.

The superior head of the lateral pterygoid (SHLP) originates at the sphenoid bone and inserts at the articular disk as well as the capsule of the temporomandibular joint (TMJ) [22]. The origin of the inferior head is the lateral pterygoid plate and its insertion is the condyle of the mandible [22]. A detailed model of the lateral pterygoid muscle is of particular interest for the understanding of temporomandibular joint disorders (TMD), since part of the superior head inserts directly on the articular disk and hence is able to apply loads directly to the joint [45][46][47]. Furthermore, Murray et al. showed that an increase or decrease of activation of the LPT leads to a decreased stabilization of the TMJ [14].

To increase the understanding of the internal workings of the lateral pterygoid, Murray et al. conducted a series of EMG studies that investigated the activations of various sub-compartments of the two heads for different tasks, e.g. a contralateral movement [15][16][17][18][19][20][21]. These studies were pure EMG studies, which means that only little

reasoning on the received results was provided. To investigate a possible biomechanical explanation of the results, we developed a new lateral pterygoid model and conducted an inverse study of lateral movement.

Methods

For this chapter a new Java class was created that defines the set-up of the new lateral pterygoid model as well as all data necessary for the input and output probes.

Muscle Activations

After conducting a literature review of the anatomy, we decided to divide the superior head (SHLP) into two separate compartments and the inferior head (IHLP) into four compartments. Table 2 shows the roles we expect each compartment to fulfill, according to our literature research.

	Superomedial	Inferomedial	Superolateral	Inferolateral
IHLP	Initial phase	Fine control	Fine control	Not recorded
SHLP	Initial phase		Fine control	

Table 2: main tasks of different compartments of the lateral pterygoid during a contralateral movement

The muscle contributions during a contralateral movement can be separated into two parts:

- An initiation phase that should lead to activation in the superomedial part of the IHLP (IPSM) and the medial part of the superior head (SPM)
- A phase of fine control using the inferomedial, superolateral parts of the inferior head (IPIM, IPSL) and the lateral part of the superior head (SPL)

Figure 22 shows a schematic drawing of the sub compartments and their respective activation phases.

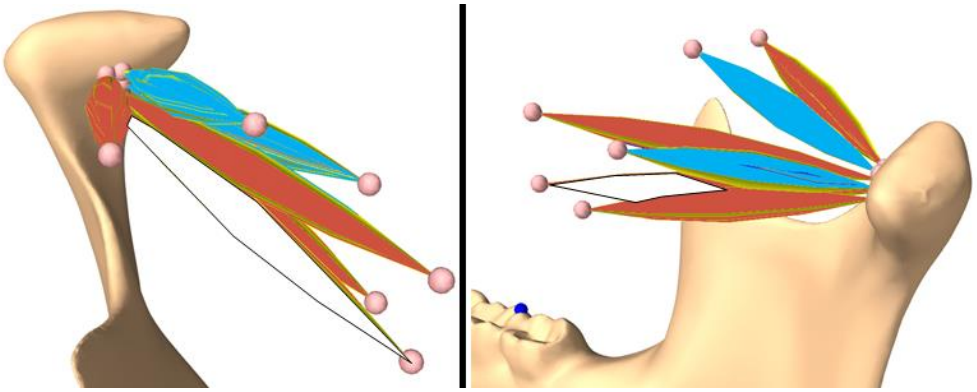

Figure 22: front and medial view of muscle compartments (blue: initial phase; brown: fine control phase)

As a first step, we tried to come up with a hypothesis that explains why this activation pattern may occur. After comparing the muscle force vectors of the two groups, we theorize that the overall force vector of the initiation phase has a substantial amount of force pulling the condyle inwards. This force presses the condyle against the skull and stabilizes the system during the initial start of the movement. After the maximum of this first activation impulse occurred, the second phase starts. The muscles of the second phase shift the overall muscle force vector to a direction that is better suited to pull the condyle forwards. This is the actual movement the right condyle has to fulfill for a left lateral movement of the mandible. Figure 23 shows a schematic drawing of our theory.

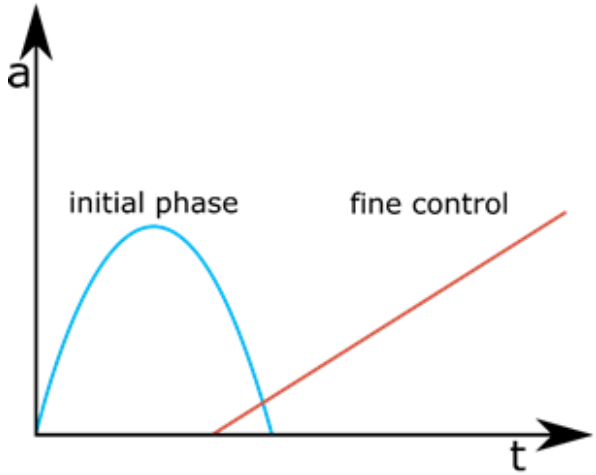

Figure 23: schematic drawing of muscle activation phases

Model

The goal of this project was to develop an inverse simulation of a left lateral movement using a new lateral pterygoid model in ArtiSynth. To create our model we used the Hannam et al. model as a basis [1]. The left temporomandibular joint was modelled using three planar constraints, while only one planar constraint was used for the right TMJ. This means that our constraint setup only allows rotation of the left condyle and translation, on the plane pictured in figure 24, for the right condyle.

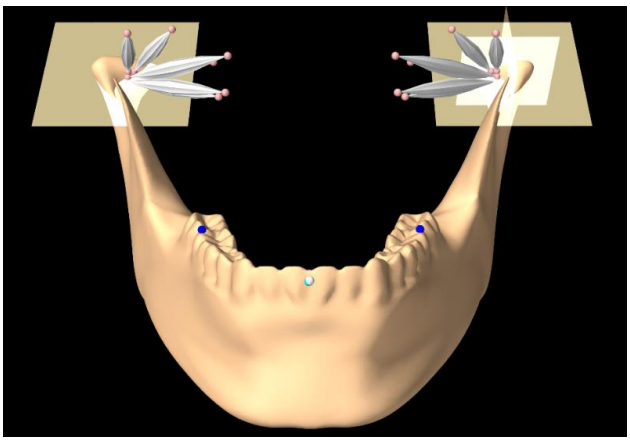

Figure 24: model set-up

To model the different compartments of the LPT, we created four point-to-point muscles for the IHLP and two point-to-point muscles for the SHLP. To produce appropriate muscle forces, one fourth of the maximum muscle force of the inferior head was used as new maximum force for all four compartments of the head, as well as half the maximum force for the two compartments of the superior head. All other muscles of the masticatory system are not included in our simulation, since we are solely interested in the workings of the lateral pterygoid muscle.

Movement Pattern and Simulation Properties

For this study, we used a movement goal that lead to a 9mm translation in x-direction, with a slight translation in y- and z- plane to fit the movement behavior of the constraint set-up above.

Due to the fact, that we are only including the lateral pterygoid muscle in our model we excluded gravity, since it would be impossible to keep the mandible at a stable height during a lateral movement without the use of some of the closing muscles of the jaw region. All investigations were done using a frame damping of 0.01 Ns/m and a rotational damping of 0.001 Ns/m for the mandible.

To investigate the effect of different regularization terms, we simulated the movement using an L1- as well as an L2- regularization term. Since the inverse controller of ArtiSynth cannot solve while only using an L1 regularization term, as described in chapter 2, an L2-regularization term with a weight of $1x10^{-9}$ was added for the L1 regularization case.

Results

L1-Regularization

To investigate the influence of the weight of the L1- regularization term, we varied its value from 0.1 to 0.01 and repeated the simulations. Figure 25 shows the muscle activation patterns for 3 investigations. No results showed agreement with the expected behavior.

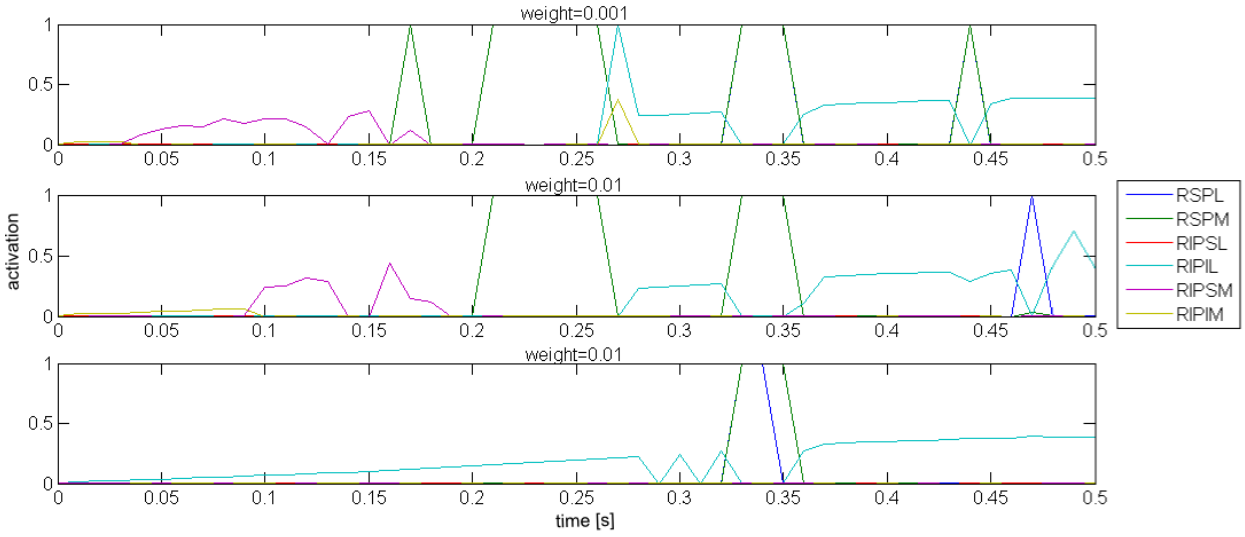

Figure 25: activation pattern using different weights for the L1- regularization terms; RIPIL – right inferior head inferolateral part; RIPIM – right inferior head inferomedial part; RIPSL – right inferior head superolateral part; RIPSM – right inferior head superomedial part; RSPL – right superior head lateral part; RSPM – right superior head medial part

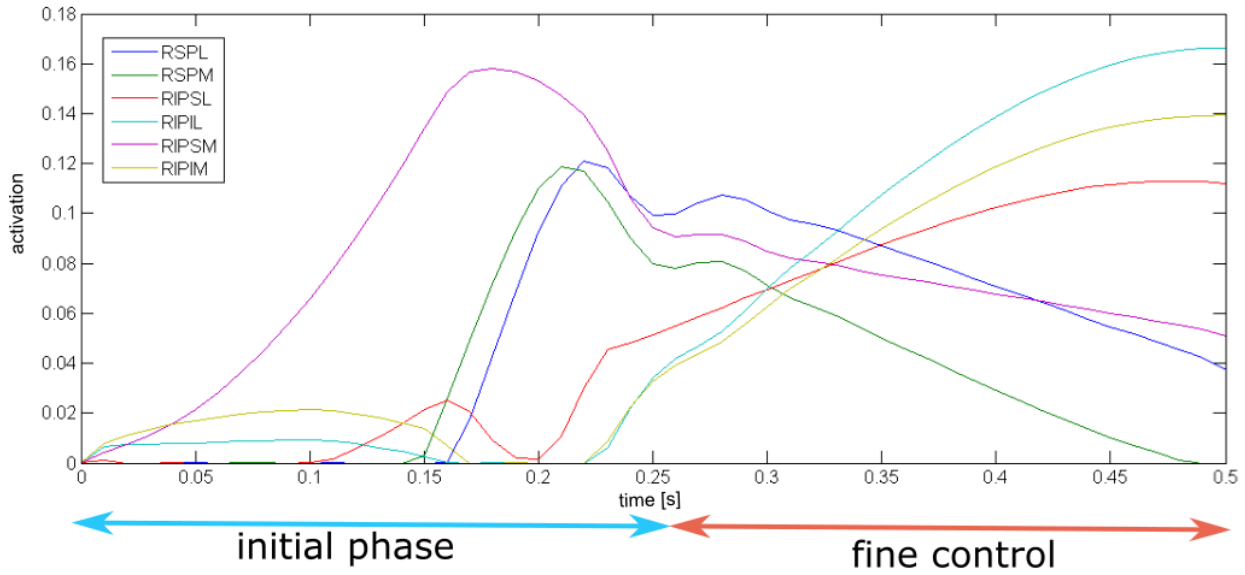

Figure 26: muscle activation pattern for left lateral movement using L2-regularization (time in seconds). RIPIL – right inferior head inferolateral part; RIPIM – right inferior head inferomedial part; RIPSL – right inferior head superolateral part; RIPSM – right inferior head superomedial part; RSPL – right superior head lateral part; RSPM – right superior head medial part

L2-Regularization

Figure 26 shows the results for the simulation using an L2- regularization term with a weight of 0.1. In general the pattern is separated into two parts. The first part contains the superior medial part of the right IHLP as well as the medial and lateral part of the SHLP. After the initial phase starts decreasing, the second part of activation, consisting of the inferomedial IHLP, the superolateral IHLP and the inferolateral IHLP, starts to increase.

Discussion

Using a L1- regularization term did not produce results that were in accordance with literature. This is most likely due to the tendency of a L1- regularization to activate one muscle strongly instead of spreading the activation over multiple muscles. This behavior can be seen in figure 25 where an increase of the weight of the term reduces the number of activated muscles. For the simulations with a lower weight, the regularization term is too "weak" to effectively work and hence the simulation produces short activation spikes that increase with smaller weights. Since we are looking for a muscle activation pattern that spreads activation over multiple compartments, a L1- regularization term is not a feasible tool.

In general the results for the muscle activation patterns using an L2-regularization term showed a better agreement with the EMG studies. Figure 26 shows the best fit, using a weight of 0.1. Higher weights will slowly make it harder for the simulation to follow the movement goal, due to its reduced relative importance, and lower weights will reduce the spreading of activation and will lead to short spikes of activation, similar to the results using a low weight for the L1 regularization term.

According to literature, muscle activations for a contralateral movement should be separated into an initial and a fine control part. The same behavior can be seen in figure 26. The

first group contains the muscles that were expected, with an additional activation of the lateral part of the SHLP. The muscles of the second group were in agreement with literature again except for the lateral part of the superior head, which was used for initiation. Furthermore, the inferolateral part of the IHLP was used, but we were not able to find any data on its role during a lateral movement, but looking at its muscle force vector, it could be well suited for this task.

In summary, we can say that our inverse simulation results, using an L2-regularization term, show that the biomechanical properties of the model suggest a muscle activation pattern consisting of two parts. The use of an L2-regularization term makes sense, since EMG studies suggest an activation pattern that is spread out over all sub-compartments of the muscle.

Moreover, the simulation grouped the muscles the same way that they were activated in the EMG studies except for a single compartment, the lateral part of the SHLP. A possible reason for this difference could be that, in our model, the lateral part of the SHLP seems to have the best muscle force vector to protrude the mandible from rest position, which makes this compartment well suited for the translation of the condyle in earlier stages. To investigate this discrepancy in future work, we plan to go back and verify the positions of the insertions and origins for the muscle compartments with the help of an expert.

CHAPTER 6:
TOWARDS AN OPENSIM MODEL OF THE JAW REGION

Introduction

Even though musculoskeletal models of the masticatory system have been developed in a number of simulation environments their accessibility is quite poor, since most of these models are developed using commercial software, like Matlab [2], AnyBody [3] and Madymo [9]. Using one of these models would already introduce a big financial burden at the beginning of the project. This makes it hard for new research groups to start working in the field of orofacial biomechanics and hence slows down the discovery of new insight into the workings of the masticatory system.

To increase the number of biomechanical studies of the jaw region, we propose to develop a jaw model using OpenSim. OpenSim is a freely available multibody simulation toolkit for musculoskeletal simulations. It has thousands of users around the world, with a strong focus on lower limb models and simulations [10][48][49].

OpenSim offers muscle models that include properties not present in previous models (activation dynamics, tendon compliance, et al.) so it will be interesting to evaluate the effect of these properties on simulations for a model of the masticatory system in OpenSim.

Although OpenSim is the most used musculoskeletal modeling toolkit, and its SimTK.org repository has over 100 models available, it is currently lacking a model of the masticatory system. Building a jaw model in OpenSim would provide a tool to the SimTK community for analyzing masticatory biomechanics and help to encourage the adoption of musculoskeletal

modeling in clinical dentistry. To create this model, we sought to port the Hannam et al. 2008 model that was originally developed using ArtiSynth and additionally is publicly available [1]. For this purpose, we came up with possible ways to port the muscle properties from ArtiSynth, as well as ways to model the temporomandibular joint using OpenSim's joint approach.

The first difficulty was the difference in programming language between the two toolkits, since ArtiSynth models are programmed using Java, while OpenSim is using C++ and the architectures of the two languages are sufficiently different that one cannot simply port models directly.

OpenSim is using an internal coordinate approach, in contrast to the world coordinates used in ArtiSynth. This means we had to come up with a new representation of the temporomandibular joint, since the representation used in ArtiSynth was not applicable in OpenSim.

Lastly, OpenSim is using a different muscle model than ArtiSynth. To make the OpenSim model behave in a similar manner to the ArtiSynth model we had to find a way to port the muscle properties to OpenSim's muscle model.

Methods

The specific aim of this study was to port the Hannam et al. jaw model to OpenSim. This model was originally implemented using the ArtiSynth toolkit and has been used in a number of simulation studies related to mastication. By implementing this state-of-the-art jaw model in OpenSim, we are able to use its unique analysis features, such as induced acceleration analysis, and computer muscle control.

To develop the model, we created a C++ project, using the OpenSim and SimTK libraries. This method enabled us to control and adjust all aspects of the model very easily.

Geometry

Since the goal of the project was to create a jaw model that is as similar to the Hannam et al. model as possible we used the same geometry data and insertion point files that were used for the bony structures and muscles attachments in ArtiSynth.

Muscle Properties

ArtiSynth uses a muscle model that is not provided in OpenSim. The most used muscle model in OpenSim is the Millard Equilibrium Musculotendon Model [50]. The default setup for this muscle model uses a spring as a tendon representation, but since the tendons of the muscles of the masticatory system are short tendons, we can assume rigid tendons.

To initialize a Millard muscle, we need the following input variables:

- maximum force of muscle
- optimal fiber length
- tendon slack length
- pennation angle

The tendon slack length is defined as the length at which further stretching would introduce spring forces. In our model, we are using a rigid tendon, hence in our case the tendon slack length is simply the maximum length of the tendon. This means that the muscle length is computed by:

$$l^{MT} = l^{T} + l^{M} \cos \alpha \qquad (1)$$

where l^{MT} is the length of the musculotendon complex, l^T the length of the tendon, l^M the length of the muscle and α is the pennation angle, which is the angle between the tendon and muscle fiber.

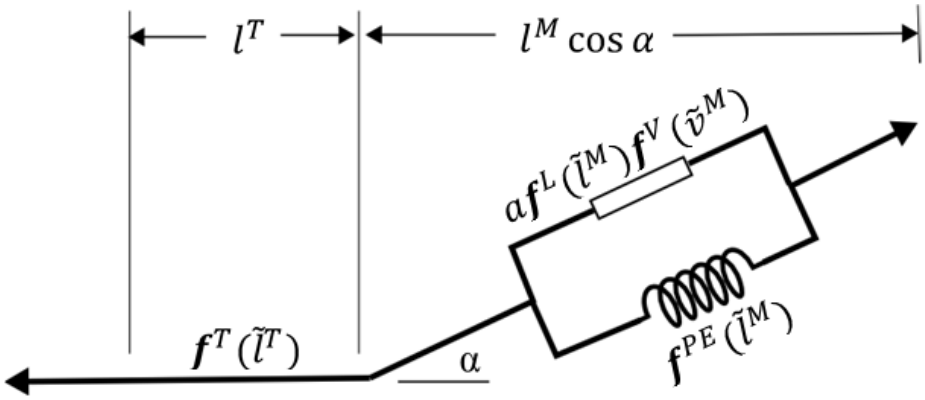

Figure 27: schematic drawing of the muscle model used

We found the maximum force, optimal fiber length and pennation angle for all jaw muscles in literature [51]. Unfortunately we could not find any information on tendon length, hence we had to come up with a workflow that allows us to use the literature data for the maximum force and pennation angle to find an estimation for all biomechanical properties of the individual muscles.

In a first step we have to make an estimation of the tendon slack length. For this purpose we took 10% of the length of every muscle at closed mouth position in ICP. In the next step, we recorded the length of every muscle after we ran a simulation of a passive mouth opening without any muscle excitation.

For a modeling purpose, we can assume that at a passive opening the tendons length will be the tendon slack length and muscle fibers have not stretched yet and hence still will be at the optimal fiber length. Using the pennation angles gathered from literature we now can compute the optimal fiber length of a specific muscle using:

$$l_{opt}^{MF} = \frac{l_p^M - l_{sl}^T}{\cos \alpha} \quad (2)$$

,where l_p^M is the length of the muscle after passive opening, l_{sl}^T is the tendon slack length and α is the pennation angle.

Joint Representation

One of the major difficulties during the course of this project was to find a joint representation in OpenSim that mimics the behavior of the Hannam et al. model. ArtiSynth is using a full coordinate approach and three unilateral constraints for each of the temporomandibular joints. On the other hand, OpenSim is using internal coordinates, which means that a new body is defined in terms of its parent body and joint that connects the parent with the new child body. Furthermore a parent and a child body can only have one joint connecting the two. Additionally, you need to allow degrees of freedom in OpenSim, while ArtiSynth needs you to restrict degrees of freedom.

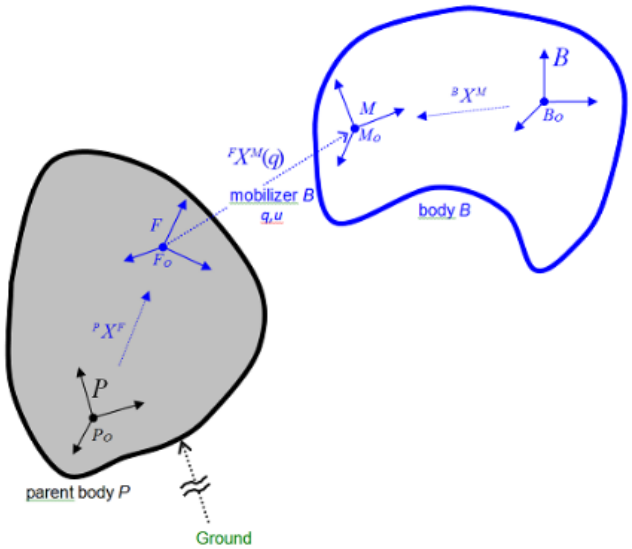

Figure 28: model hierarchy in OpenSim (connecting a parent body and a child body using a mobilizer) [52]

OpenSim lets you define a function for every degree of freedom, which will give you a transformation that defines how the child body can move over time. Figure 28 shows the model hierarchy in OpenSim.

OpenSim allows only one joint between parent and child body, which leads to difficulties since the jaw and the skull are anatomically connected by two joints. Especially the lateral movement of the jaw, which depending on the direction of movement will have a rotational center in one condyle while the other condyle is translating, is hard to model with one joint since the simulation would have to make the joint change its position, between the positions of the two condyles, during the course of the simulation, which is not possible in OpenSim.

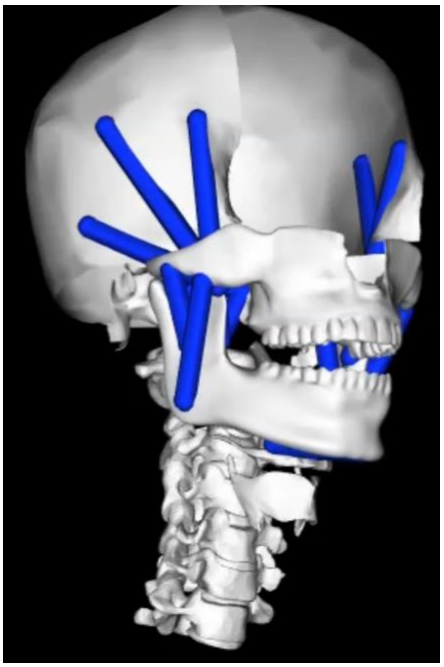

Figure 29: screenshot of the model with attached muscles

We tested different approaches to develop a joint model that enables us to test the muscle properties described above and overcome the problems occurring due to the internal coordinate method.

Two Degree of Freedom Joint

As a first model we used one custom joint, sitting in the middle between the two condyles. We enabled rotation around the x-axis, for opening, and translation in y- and z-direction, using a cubic function, for protrusion. This model was set up using the muscle properties described earlier.

Saloon Door Joint

The second joint model was inspired by one of the mechanisms that enables doors to open in both directions, often seen in libraries or old western saloons.

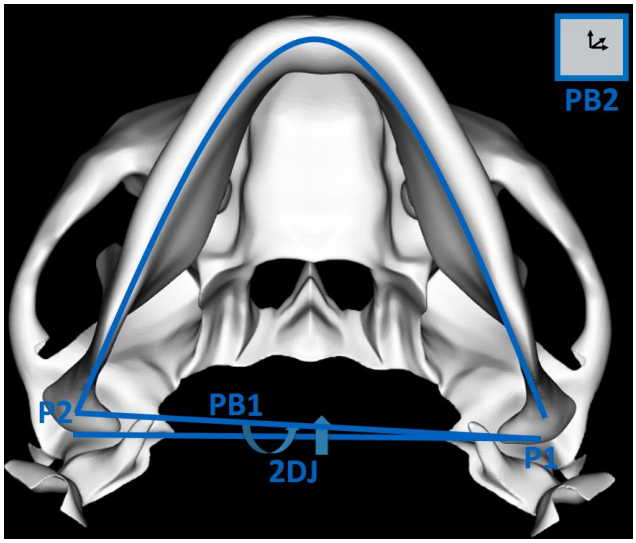

Figure 30: schematic drawing of bodies and joints for the saloon door model; P1/ P2: pinjoint 1 and 2; 2DJ: two degree of freedom joint; PB1/ PB2: phantom body 1 and 2

From a modeling point of view these joints consist of a pinjoint, connecting the doorframe with a thin connection body and a second pinjoint, connecting the connection body with the actual door. Depending on the direction from which force is applied to the door one pinjoint will open while the other one stays closed, which will lead to rotation at one pinjoint and translation of the other. Using a phantom body, which is a body without mass and no attached

geometry, for the connection body and placing one pinjoint in each condyle, we get the model setup shown in figure 30.

To make sure that both pinjoints are never opened at the same time, we added another phantom body to get an additional degree of freedom we could use to connect the two pinjoints. This was done using two CoordinateCouplers that connect the first pinjoint's coordinate to the phantom body using a function that is zero while the coordinate of the phantom body is negative and increases linearly when it is positive. For the other pinjoint, the coupling function is zero during the positive part of the coupled coordinate and increases once the coordinate becomes negative. This way we make sure that only one pinjoint angle is non zero at the same time. By combining this joint with the simple 2 degree of freedom joint, described earlier, we get a setup that is able to open, protrude and move laterally.

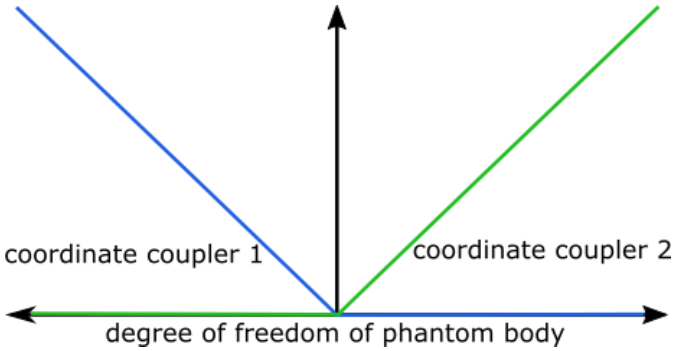

Figure 31: schematic drawing of the two coordinate couplers that ensure that only one pinjoint is opened at the same time

Results

Two Degree of Freedom Model

Figure 32 shows two simple simulations that were computed using the two degree of freedom model. While pictures a) and b) show the resting state, without any muscle activation, pictures c) and d) depict an activation of both heads of the masseter, which leads to a closing of the mouth. In picture e) and f) both heads of the lateral pterygoid, the anterior digastric and the

geniohyoideus muscle are activated on both sides of the jaw. This leads to a maximum opening of the jaw, which is accomplished by protrusion of the condyles and rotational opening. The maximal opening of the model was measured at 44.6 mm and passive opening was measured as 11.3 mm. The muscle properties used for these simulations can be found in Appendix A.

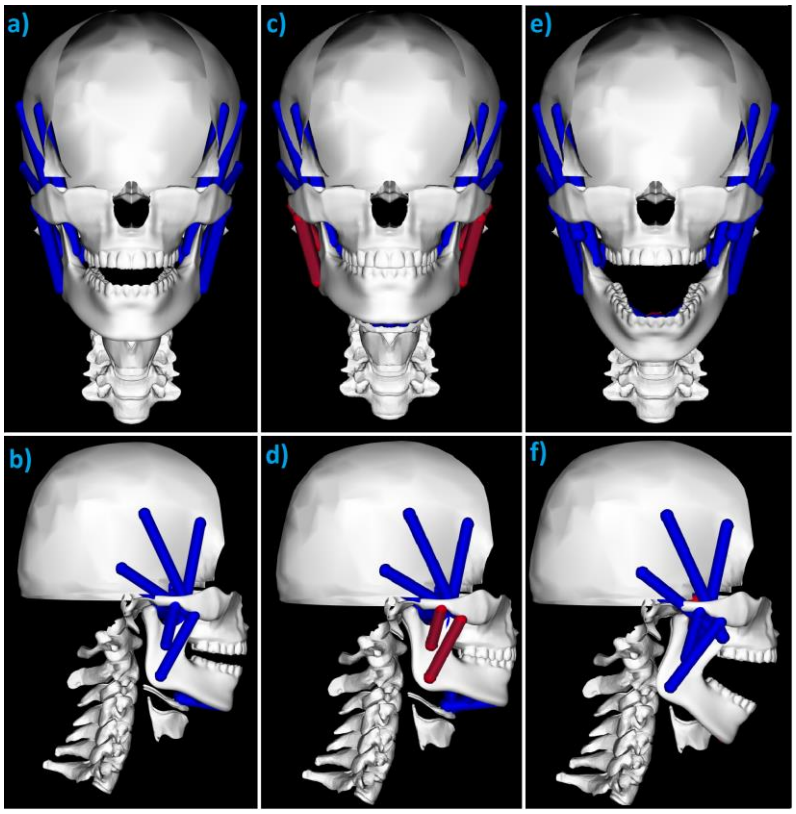

Figure 32: a) frontal view of passive opening, b) side view of passive opening, c) frontal view of closed jaw, d) side view of closed jaw, e) frontal view of open jaw, f) side view of open jaw

Saloon Door

Using the setup described earlier, we were able to create a temporomandibular joint that is able to move laterally. We combined this model with the two degree of freedom model, which enables the jaw to rotate, translate forward and move laterally. Figure 34 shows a variety of movements that can be performed using this joint. Due to problems with the coordinate coupler (see Discussion section), this model currently cannot be driven by muscle forces. Hence we used the coordinates of the joint (figure 33) to create the result plots.

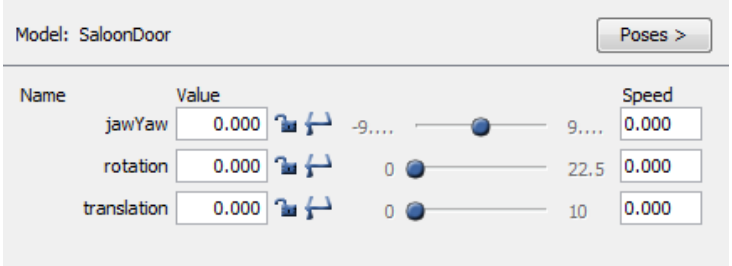

Figure 33: coordinates that are used to define jaw movement of the combined two degree of freedom and saloon door model

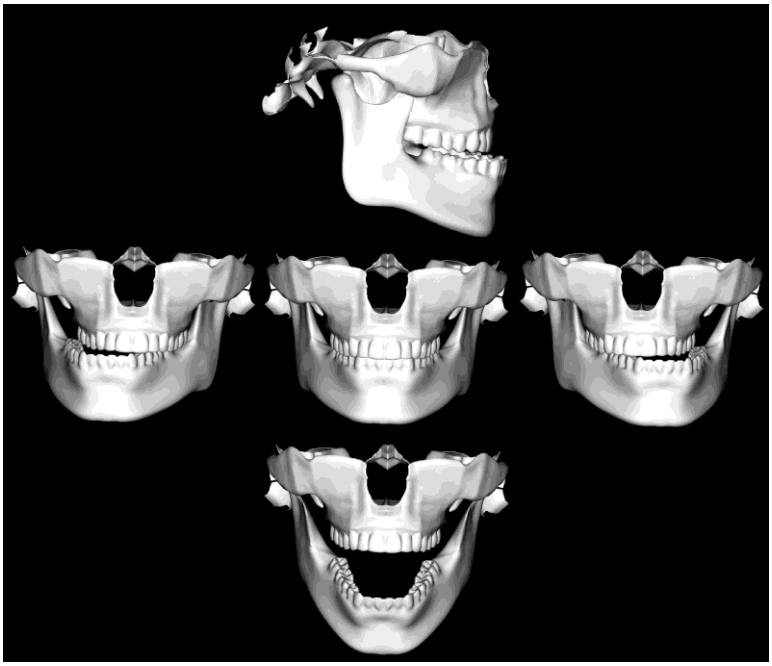

Figure 34: possible movements using a jaw model that combines the two degree of freedom joint with a saloon door joint

Discussion

During the course of this project we encountered several problems due to the differences between ArtiSynth and OpenSim.

The first difficulty was to set up the muscle properties in a way that keeps them as close as possible to literature, while enabling similar simulation results as observed in ArtiSynth. As described above, we had to come up with a more or less arbitrary tendon slack length due to the lack of published tendon data. This was not a problem in ArtiSynth, due to the fact that the

muscle model in ArtiSynth doesn't include a tendon. Furthermore we had to change the optimal fiber length to come up with realistic muscle dynamics.

Since our main goal is not necessarily to be as close to literature as possible, but to mimic the behavior of the Hannam et al. model, which has been validated before, it is reasonable to slightly alter the literature values to get more comparable results. Furthermore, the optimal fiber length of the Hannam et al. model was altered as well to increase the performance of the model [1]. The results of some simple simulations performed with this model suggest that our way of setting up the muscle properties seems to work quite well. The maximal opening of the mouth was 44.6 mm which is in between the 38mm maximal gape in a simulation using a similar setting in ArtiSynth and the actual literature value of 50mm. The resting position, with an opening of 11.3mm, is not in the range of normal human rest opening, which would be between 3-5 mm. This is a problem that already occurred in ArtiSynth, where a small activation of 0.04% in the closer muscles is used to achieve the correct rest position. This activation only leads to a decrease of the gap to 10.6mm. To compute a reasonable passive opening gap, an activation of 0.2% has to be used to get an opening of 3.8mm.

One of the biggest challenges during this project was the difference in coordinate systems used in the two toolkits. Many ideas that are used to set up the joints in ArtiSynth are straightforward and easy to implement with a full coordinate system, but are not feasible for an internal coordinate approach. The best example for this problem is the lateral movement of the mandible. In ArtiSynth the mandible will just leave the posterior constraint for translation forwards and inwards on one side, while the other condyle cannot penetrate the constraint and therefore has to start rotating.

By using internal coordinates, you would have to make the center of rotation switch between the two condyles depending on the position of the jaw, which is not possible. This means we had to come up with another, quite complicated, way to enable this movement, which was easily accomplished in ArtiSynth.

To solve these limitations we developed a representation that we called the saloon door joint. This joint transfers the mechanisms of a double acting hinge to the realm of biomechanics. By combining the saloon door joint with the simple two degree of freedom joint, described above, we enable the simulation to perform all possible movements of the jaw.

Future work will aim to work on some of the present limitations of the model. Currently we are still using piecewise linear functions to set up the coordinate couplers, which means we are not able to run simulations with this model. To fix this, we would need to use continuous functions instead. By using continuous functions we would have the problem that at a zero value of the coordinate of the phantom body, which is used for the coupling, both pinjoints will be opened slightly. At this point, we cannot say if this would just lead to a very small error or would be a major problem of the model.

Furthermore, the saloon door joint is strictly translating forward, in contrast to the translation along the articular surface (which we mimicked using a cubic function of y and z in the 2D model). To set up a correct translation, we would have to use a custom joint instead of the pinjoint and define proper functions for the rotations around all three axes.

CHAPTER 7:
SUMMARY & FUTURE WORK

This thesis presented a set of biomechanical simulation projects focused on the human jaw region. Projects included the development of new optimization methods as well as the creation of new models for specialized simulations of different settings. This chapter will give an overview of the author's contributions to the projects presented in this thesis. Moreover we will highlight potential future research tasks that would improve the performance or clinical relevance of the presented projects.

Contributions

The main contributions of this thesis were the development of a reaction force optimization term for inverse simulations, a detailed model of the sub compartments of the lateral pterygoid muscle, a specialized jaw model for the investigation of sleep bruxism and an OpenSim representation of the Hannam et al. model.

Reaction Force Goal

We developed a new quadratic optimization term that enabled us to run inverse simulations in ArtiSynth that could use a predefined level of constraint reaction force. This term can be combined with a previously developed movement goal to receive muscle activation patterns for tasks that are composed of a movement and a substantial amount of force that is not

used for movement itself (e.g. bite force). This enables the user to investigate effects of various force levels on systems for which measuring reaction forces is not possible without interfering with the system itself. To the best knowledge of the author this is the first simulation set-up using movement as well as reaction force for optimization.

Detailed Lateral Pterygoid Model

After reviewing the literature on the activation of the lateral pterygoid muscle during a contralateral movement, we developed a biomechanical theory to try to explain the reported activation patterns, since previously only little explanation has been presented. Using a newly developed lateral pterygoid model, we ran inverse simulations of contralateral movement and could show that the simulation results were in quite good agreement with our theory and reported EMG patterns.

Inverse Simulations of Sleep Bruxism

We created a specialized model for investigations of sleep bruxism. Using a movement as well as a reaction force goal, we could achieve realistic muscle activation patterns for grinding movements. Our results show general agreement with literature, except for the activation of the submental muscles, which was expected due to the optimization method chosen.

OpenSim Model

Lastly, we investigated multiple ways to transfer the Hannam et al. model from ArtiSynth to OpenSim to drastically increase its availability. We had to come up with a way to port the muscle properties from ArtiSynth to OpenSim since both toolkits are using different muscle

models. The second contribution of this project was to develop a novel model of the temporomandibular joint using an internal coordinate approach.

Future Work

There are multiple research ideas that could build on the work presented in this thesis. This includes the creation of more detailed models of various parts of the anatomy, the improvement of approaches presented in this thesis as well as the utilization of the reaction force goal for problems of a different anatomical region. Here we propose a few promising directions for possible future projects.

Incorporating Unilateral Constraints into the Inverse Solver

As of now, unilateral constraints are not supported by the inverse solver in ArtiSynth. For forward simulations, the TMJ is modeled as a combination of unilateral constraints, which is not feasible for inverse dynamics investigations. Using only bilateral constraints, the movement of the condyles is strongly limited, hence the incorporation of unilateral constraints could improve the accuracy of results for inverse dynamics simulations.

Development of a Stiffness Optimization Term

Our bruxism simulation was not able to recruit the submental muscles during teeth clenching, since these opening muscles act against the primary movement and hence are not selected with the current optimization set up. Coactivation of antagonistic muscles will most likely increase the stiffness of the system. By adding a stiffness term to the optimization we could enable the simulation to activate antagonistic muscles to meet a predefined stiffness goal.

Reevaluation of the Muscle Property Porting Method

While the maximal opening of the OpenSim model is actually closer to the literature, its passive opening simulation yields a quite large gap. Future steps should include a reevaluation of the method used to port the properties and running further tests. This should show if the difference in performance is caused by the porting method or solely by the differences in muscle models, e.g. representation of tendon dynamics.

Saloon Door Joint

The approach of using a double acting hinge to model the lateral movement of the mandible showed big promise. Further steps should include the use of continuous functions for the coordinate coupler to enable the user to run dynamic simulations. Furthermore, the pinjoints should be replaced by custom joints with translation and rotation functions that appropriately mimic the movement of the contralateral condyle along the articular surface.

Implementation of a Unilateral Constraint in OpenSim

Since most major problems with our OpenSim model stem from the lack of a method to define a simple joint representation an implementation of a unilateral constraint could solve a lot of problems easily. Unilateral constraints would enable us to set up the same joint we use in ArtiSynth, which is easy to create and mimics the actual bony structures around the condyle, hence we could solve these problems while using an anatomically meaningful solution.

Model Validation

To strengthen the results presented in this thesis a series of experimental measurements could be done. Possible experiments include the recording of EMG of sleep bruxism, to validate

the core results of the project. For example measuring the temporalis muscle, for multiple patients, could show if the alternating higher amplitude is a regular occurrence. If mandible movement would be collected simultaneously it could be shown if the unilateral activation is actually used to pull the mandible inwards or outwards respectively.

Additionally conducting a cadaver study would enable us to collect tendon data, which could be used to set up the OpenSim muscle model without the extra step of changing the properties.

Summary

We have presented a new optimization term that uses constraint reaction forces, which was thereafter used to develop an inverse simulation of sleep bruxism. Furthermore a new, detailed model of the lateral pterygoid model was created and used to investigate possible biomechanical reasons for its activation pattern during a contralateral movement. To increase the availability of jaw models to the research community, we examined ways to bring the ArtiSynth jaw model to the OpenSim modeling community.

LIST OF REFERENCES

[1] Hannam AG, Stavness I, Lloyd JE, and Fels S. A dynamic model of jaw and hyoid biomechanics during chewing. J Biomech 2008; 41: 1069-1076.

[2] Tuijt M, Koolstra JH, Lobbezoo F and Naeije M. Differences in loading of the temporomandibular joint during opening and closing of the jaw. Journal of biomechanics 2010; 43(6): 1048-1054.

[3] De Zee M, Dalstra M, Cattaneo PM, Rasmussen J, Svensson P and Melsen B. Validation of a musculo-skeletal model of the mandible and its application to mandibular distraction osteogenesis. Journal of biomechanics 2007; 40(6): 1192-1201.

[4] Ingawale S. and Gowami T. Temporomandibular Joint: Disorders, Treatments, and Biomechanics. Annals of Biomedical Engineering 2009; 37(5): 976–996.

[5] Carra MC, Huynh N and Lavigne G. Sleep bruxism: A comprehensive overview for the dental clinician interested in sleep medicine. Dent Clin North Am 2012; 56: 387-413.

[6] Castroflorio T, Bracco P and Farina D. Surface electromyography in the assessment of jaw elevator muscles. J Oral Rehabil 2008; 35: 638-645.

[7] Bakke M, Michler L, Han K and Möller E. Clinical significance of isometric bite force versus electrical activity in temporal and masseter muscles. Scandinavian Journal of Dental Research 1989; 97: 539-551

[8] Hannam AG. Current computational modelling trends in craniomandibular biomechanics and their clinical implications. Journal of Oral Rehabilitation 2010; 38(3): 217-234

[9] Koolstra JH and van Eijden TM. Combined finite-element and rigid-body analysis of human jaw joint dynamics. Journal of Biomechanics 2005; 38: 2431-2439

[10] Delp SL, Anderson FC, Arnold AS, Loan P, Habib A, John CT, Guendelman E and Thelen DG. OpenSim: Open-source Software to Create and Analyze Dynamic Simulations of Movement. IEEE Transactions on Biomedical Engineering 2007; 54(11): 1940 – 1950.

[11] Stavness I, Hannam AG, Lloyd JE, and Fels S. Predicting muscle patterns for hemimandibulectomy models. Comput Methods Biomech Biomed Engin 2010; 13: 483-491.

[12] Murray GM, Bhutada M, Peck CC, Phanachet I, Sae-Lee D and Whittle T. The human lateral pterygoid muscle. Arch. Oral Biol. 2007; 52: 377-380

[13] Davies J, Charles M, Cantelmi D, Liebgott B, Ravichandiran M, Ravichandiran K, and Agur A. Lateral pterygoid muscle: A three-dimensional analysis of neuromuscular partitioning. Clinical Anatomy 2011; 25: 576-583.

[14] Murray GM, Phanachet I, Uchida S and Whittle T. The role of the human lateral pterygoid muscle in control of horizontal jaw movements. J Orofac Pain 2001; 15: 279-305

[15] Uchida S, Whittle T, Wanigaratne K and Murray G.M. The role of the inferior head of the human lateral pterygoid muscle in the generation and control of horizontal mandibular force. Arch Oral Biol, 2001: 46: 1127–1140

[16] Uchida S, Whittle T, Wanigaratne K and Murray G.M. Activity in the inferior head of the human lateral pterygoid muscle with different directions of isometric force. Arch Oral Biol, 2002; 47: 771–778

[17] Uchida S, Whittle T, Wanigaratne K and Murray G.M. Functional properties of single motor units in inferior head of human lateral pterygoid muscle: task relations and thresholds. J Neurophysiol, 2001; 86: 2204–2218

[18] Uchida S, Whittle T, Wanigaratne K and Murray G.M. Functional properties of single motor units in the inferior head of human lateral pterygoid muscle: task firing rates. J Neurophysiol, 2002; 88: 751–760

[19] Phanachet I, Whittle T, Wanigaratne K, Klineberg I.J, Sessle B and Murray G.M. Functional heterogeneity in the superior head of the human lateral pterygoid J Dent Res, 2003; 82: 106–111

[20] Ruangsri S, Whittle T, Wanigaratne K and Murray G.M. Functional activity of superior head of human lateral pterygoid muscle and isometric force. J Dent Res, 2005; 84: 548–553

[21] Sae-Lee D, Wanigaratne K, Whittle T, Peck C.C and Murray G.M. A method for studying jaw muscle activity during standardized jaw movements under experimental jaw muscle pain. J Neurosci Meth, 2006;157 285–29

[22] Drake R, Vogl AW and Mitchell AWM. Gray's Anatomy for Students. Elsevier Ltd, Oxford, 2010

[23] http://www.daviddarling.info/encyclopedia/T/teeth.html

[24] The glossary of prosthodontic terms. J Prosthet Dent 2005; 94(1):10–92.

[25] Lavigne GJ and Montplaisir JY. Restless legs syndrome and sleep bruxism: prevalence and association among Canadians. Sleep 1994; 17(8): 739-743.

[26] Simola P, Niskakangas M, and Liukkonen K. Sleep problems and daytime tiredness in Finnish preschool-aged children-a community survey. Child Care Health Dev 2010; 36(6): 805-811.

[27] Lavigne GJ, Rompré PH, Poirier G, Huard H, Kato T and Montplaisir JY. Rhythmic Masticatory Muscle Activity during Sleep in Humans. Journal of Dental Research 2001; 80: 443-448

[28] American Academy of Sleep Medicine (AASM). International classification of sleep disorders. Diagnosis and coding manual. (ICSD-2). Section on sleep related bruxism. 2nd edition. Westchester (IL): American Academy of Sleep Medicine; 2005: 189-192.

[29] Lavigne GJ, Manzini C and Kato T. Sleep bruxism. In: Kryger MH, Roth T, Dement WC, editors. Principles and practice of sleep medicine, 4th ed. Philadelphia: Elsevier Saunders, 2005: 946-959.

[30] Greaves WS. The jaw lever system in ungulates: a new model. J Zool 1978; 184: 271-285.

[31] Throckmorton GS and Throckmorton LS. Quantitative calculations of temporomandibular joint reaction forces - I. The importance of the magnitude of the jaw muscle forces. J Biomech 1985; 18: 445-452.

[32] Röhrle O and Pullan AJ. Three-dimensional finite element modelling of muscle forces during mastication. Journal of Biomechanics 2007; 40: 3363-3372

[33] Lloyd JE, Stavness I, and Fels S. ArtiSynth: A fast interactive biomechanical modeling toolkit combining multibody and finite element simulation. 2012; 11: 355-394.

[34] Langenbach GEJ and Hannam AG. The role of passive muscle tensions in a three-dimensional dynamic model of the human jaw. Archives of Oral Biology 1999; 44: 557-573.

[35] Peck CC, Langenbach GEJ and Hannam AG. Dynamic simulation of muscle and articular properties during human wide jaw opening. Archives of Oral Biology 2000; 45: 963-982.

[36] Hill AV. Mechanics of active muscle. Proceedings Royal Society 1953; 141: 104–117

[37] Ng AY. Feature selection, L1 vs. L2 regularization, and rotational invariance. Proceedings of the 21st International Conference on Machine Learning 2004;

[38] Qiao X. Variable selection using Lq penalties. WIREs Comput Stat 2014; 6: 177-184

[39] Saul KR, Hu X, Goehler CM, Daly M, Vidt ME, Velisar A and Murray WM. Benchmarking of dynamic simulation predictions in two software platforms using an upper limb musculoskeletal model. Comput Methods Biomech Biomed Engin 2015; 18(13): 1445-1458

[40] Douglas WH, Sakaguchi RL, and DeLong R. Frictional effects between natural teeth in an artificial mouth. Dental Materials 1985; 1: 115-119.

[41] Zheng J, Zhou ZR, Zhang J, Li H and Yu HY. On the friction and wear behavior of human tooth enamel and dentin. Wear 2003; 255: 967-974.

[42] Zheng J and Zhou ZR. Friction and wear behavior of human teeth under various wear conditions. Tribology International 2007; 40: 278-284.

[43] Kato T, Masuda Y, Yoshida A and Morimoto T. Masseter EMG activity during sleep and sleep bruxism. Archives Italiennes de Biologie 2011; 149:478-491.

[44] Hogan N. Adaptive Control of Mechanical Impedance by Coactivation of Antagonist Muscles. IEEE Transaction on Automatic Control 1984; 29: 681-690.

[45] Juniper RP. Temporomandibular joint dysfunction: A theory based upon electromyographic studies of the lateral pterygoid muscle. Br J Oral Maxillofac Surg 1984; 22: 1-8.

[46] Bakke M, Møller E, Werdelin LM, Dalager T, Kitai N and Kreiborg S. Treatment of severe temporomandibular joint clicking with botulinum toxin in the lateral pterygoid muscle in two cases of anterior disc displacement. Oral Surg Oral Med Oral Pathol Oral Radiol Endod 2005; 100: 693-700.

[47] Tanaka E, Hirose M, Inubushi T, Koolstra JH, Van Eijden TM, Suekawa Y, Fujita R, Tanaka M and Tanne K. Effect of hyperactivity of the lateral pterygoid muscle on the temporomandibular joint disk. J Biomech Eng 2007; 129: 890-897.

[48] Hamner SR, Seth A and Delp SL. Muscle contributions to propulsion and support during running. Journal of Biomechanics 2010; 43/14): 2709-2716.

[49] Delp SL, Loan JP, Hoy MG, Zajac FE, Topp EL and Rosen JM. An interactive graphics-based model of the lower extremity to study orthopaedic surgical procedures. IEEE Transactions on Biomedical Engineering 1990; 37: 757-767

[50] Millard M, Uchida T, Seth A and Delp SL. Flexing Computational Muscle: Modeling and Simulation of Musculotendon Dynamics. Journal of Biomechanical Engineering 2013; 135(2)

[51] Van Eijden TM, Korfage JA and Brugman P. Architecture of the Human Jaw-Closing and Jaw-Opening Muscles. The Anatomical Record 1997; 248, 464-474

[52] Seth, A., Sherman, M., Eastman P., Delp S. Minimal formulation of joint motion for biomechanisms. Nonlinear Dyn 2010; 62, 291-303

GLOSSARY

AD: Anterior Digastric Muscle

AM: Anterior Mylohyoideus Muscle

Anterior: In front of/ forward

AT: Anterior Temporalis Muscle

DM: Deep Masseter Muscle

EMG: Electromyography

FE: Finite Element

GH: Geniohyoideus Muscle

ICP: Intercuspal Position

IHLP: Inferior Head of the Lateral Pterygoid Muscle

ILP: Inferior Head of the Lateral Pterygoid Muscle

IPIL: Inferolateral Part of the Inferior Head of the Lateral Pterygoid Muscle

IPIM: Inferomedial Part of the Inferior Head of the Lateral Pterygoid Muscle

IPSL: Superolateral Part of the Inferior Head of the Lateral Pterygoid Muscle

IPSM: Superomedial Part of the Inferior Head of the Lateral Pterygoid Muscle

Lateral: Sideways/ on the side

LPT: Lateral Pterygoid Muscle

Medial: Towards the middle of the skull/ located close to the middle of the skull

MP: Medial Pterygoid Muscle

MT: Medial Temporalis Muscle

PM: Posterior Mylohyoideus

Posterior: Behind/ backwards

Protrusion: forwards movement of the mandible

PT: Posterior Temporalis Muscle

QP: Quadratic Program

RMMA: Rhythmic Masticatory Muscle Activation

SB: Sleep Bruxism

SHLP: Superior Head of the Lateral Pterygoid Muscle

SLP: Superior Head of the Lateral Pterygoid Muscle

SM: Superficial Masster Muscle

SPL: Lateral Part of the Superior Head of the Lateral Pterygoid Muscle

SPM: Medial Part of the Superior Head of the Lateral Pterygoid Muscle

TMD: Temporomandibular Joint Disorders

TMJ: Temporomandibular Joint

Working side: Side of the jaw that is used for tooth grinding

APPENDIX A
MUSCLE PROPERTIES USED FOR OPENSIM SIMULATIONS

The table below shows the muscle properties used for all simulations presented in Chapter 6. The original optimal fiber length values, used in ArtiSynth, are presented as well for comparison.

Table 3: muscle properties

Muscle Name	Optimal Fiber Length OpenSim [mm]	Optimal Fiber Length ArtiSynth [mm]	Tendon Slack Length [mm]	Maximum Muscle Force [N]	Pennation Angle [deg]
Anterior Temporal	86.941947	90.355000	9.035500	158.0	15.300000
Medial Temporalis	78.848455	81.511000	8.151100	95.6	13.450000
Posterior Temporalis	61.302284	63.798000	6.379800	75.6	11.600000
Superficial Massseter	48.686837	49.171000	4.917100	190.4	16.500000
Deep Masseter	29.943797	31.057000	3.105700	81.6	6.700000
Superior Lateral Pterygoid	18.394900	21.101000	2.110100	28.67	0.000000
Inferior Lateral Pterygoid	28.437720	32.366000	3.236600	66.9	1.300000
Medial Pterygoid	48.646033	50.770000	5.077000	174.8	12.000000
Posterior Mylohyoid	27.364700	32.973000	3.297300	35.4	0.000000
Anterior Mylohyoid	23.495900	29.311000	2.931100	35.4	0.000000
Anterior Digastric	34.038197	40.142000	4.014200	40.0	13.000000
Geniohyoid	28.700300	35.687000	3.568700	32	0.000000